FACULDADE DE ENGENHARIA DA UNIVERSIDADE DO PORTO

U.PORTO

FEUP FACULDADE DE ENGENHARIA
UNIVERSIDADE DO PORTO

Traction Control System for a Formula Student Type Car - A focus on PMSM control algorithm and performance

Tiago Nuno Giesta Marques

Mestrado em Engenharia Eletrotécnica e de Computadores

Supervisor: Adriano da Silva Carvalho

July 27, 2023

Resumo

Os veículos elétricos estão a tornar-se cada vez mais uma solução eficiente e eficaz devido às suas baixas emissões, baixa manutenção, possibilidade de gerar energia durante a travagem e a opção de controlo independente das rodas quando numa configuração de motor conectado diretamente à roda. Os fabricantes de automóveis encontram-se a investir em peso na pesquisa e desenvolvimento de veículos elétricos, expandindo o seu portfólio de veículos elétricos e fazendo a transição para a mobilidade elétrica.

Esta dissertação tem como foco o desenvolvimento de um sistema de controlo de tração para um veículo de competição de Formula Student ao otimizar o seu sistema de controlo. O controlo de tração tenta maximizar a tração do veículo, existindo uma diversidade de variáveis que podem influenciá-lo, como os pneus, a potência do motor e o peso total do veículo.

Foi realizada uma revisão bibliográfica relativamente ao Motor Síncrono de Ímans Permanentes utilizado, bem como os tipos de algoritmos e estratégias de controlo que poderiam ser aplicados. A escolha incidiu sobre o algoritmo de controlo vetorial combinado com a estratégia de controlo de Binário-Ângulo Constante.

No final, o sistema foi modelado e testado no programa Simulink. Com o sistema de controlo implementado num ambiente computacional, foi realizado um desenvolvimento adicional, otimizando os ganhos do controlador de modo a tentar obter um sistema capaz de responder o mais rápido possível com precisão.

Palavras chave: Motor Síncrono de Ímans Permanentes, Controlo Vetorial, Sistema de Controlo de Tração, Algoritmo de Controlo, Estratégias de Controlo, Optimização

ii

Abstract

Electric vehicles are becoming an efficient and effective solution due to their low emissions, low maintenance, the possibility to regenerate energy when braking, and the option to have independent wheel control with an in-wheel motor configuration. Automotive manufacturers are investing heavily in electric vehicle research and development, expanding their electric vehicle portfolio, and transitioning towards electric mobility.

This dissertation will focus on designing a traction control system for a formula student vehicle, by optimizing its control system. Traction control tries to maximize the vehicle's traction and has a diversity of variables that can influence it, such as the tires, the engine power, and the vehicle's overall weight.

A literature review was conducted on the Permanent Magnet Synchronous Motor used, as well as the types of control algorithms and strategies that could be used. The choice rested in Field Oriented Control algorithm combined with a Constant Torque-Angle control strategy.

In the end, the system was modeled and tested in Simulink. With the control system implemented in a computational environment, further development was conducted by optimizing the controller gains to try and obtain a system that could respond as fast as possible without overshooting.

Keywords: Permanent Magnet Synchronous Motor, Field-Oriented Control, Traction Control System, Control Algorithm, Control Strategies, Optimization

Acknowledgements

Contents

List of Figures

List of Tables

Abbreviations

AC	Alternating Current
ADAS	Advanced Driver Assistance Systems
AV	Autonomous Vehicle
BSPD	Brake System Plausibility Device
CO2	Carbon Dioxide
CSC	Current Source Converters
CV	Combustion Engine Vehicle
DC	Direct Current
DTC	Direct Torque Control
DTC-SVM	Direct Torque Control with Space Vector Modulation
DSP	Digital signal processor
EV	Electric Engine Vehicle
FEUP	Faculdade de Engenharia da Universidade do Porto
FOC	Field Oriented Control
FS	Formula Student
h	hours
IGBT	Insulated gate bipolar transistor
IM	Induction machine
Kg	Kilograms
Km	kilometer
kW	kilowatt
LED	Light Emitting Diode
min	minutes
MJ	MegaJoule
ms	milliseconds
MTPA	Maximum Torque-per-Ampere
PI	Proportional Integral
PMSM	Permanent Magnet Synchronous Motor
PSO	Particle Swarm Optimization

PWM	Pulse Width Modulation
rad	radians
R-FOC	Rotating-Flux-Oriented Control
SVM	Space Vector Modulation
T	Time
TC	Traction Control
TS	Traction System
TSAC	Tractive System Accumulator Container
VDC	Voltage Direct Current
VSC	Voltage Source Converter
W	Watt

Symbols

CO_2min	Smallest mass of CO2 used by the competitor
CO_2team	Mass of CO2 used by the team
i_a	Stator coil current a
i_b	Stator coil current b
i_c	Stator coil current c
i_d	Direct axis current
i_s	Stator current
i_q	Quadrature axis current
i_α	Current along alpha axis
i_β	Current along beta axis
$i_d^\star$	Current reference in direct axis
$i_q^\star$	Current reference in quadrature axis
K_{aw_id}, K_{aw_iq}	Anti-windup gains for each axis
k	Slip ratio
$Laps_{team}$	Number of laps driven by the team being scored
$LapTotal_{T_{min}}$	Lap completed by the team which set the lowest endurance time
$LapTotal_{CO2_{min}}$	Lap completed by the team which set the lowest mass of CO2 used
L_d	Direct axis inductance
L_q	Quadrature axis inductance
P	Pole pairs
R	Stator windings resistance
r	Radius of wheel [m]
$S_a; S_b; S_c$	Binary switch
t	Time
T_e	Electromagnetic Torque
T_{min}	Lowest endurance time, including penalties
T_{team}	Combined endurance times of the drivers in one heat, including penalties
T1	Transistor 1
T2	Transistor 2

V_{an}; V_{bn}; V_{cn}	Phase output voltages
v_s	Voltage space vector
v_x	Velocity of the car [m/s]
$v_d^{unsat}, v_q^{unsat}, v_d^{sat}, v_q^{sat}$	Saturated and unsaturated voltages
$v_{d_m ax}$	Maximum voltage that does not exceed voltage phase limit
$v_{ph_m ax}$	Maximum phase voltage
w	Angular velocity of driven wheel [rad/s]
w_m	Mechanical angular velocity of the rotor [rad/s]
w_0	Angular velocity of free rolling wheel [rad/s]
μ	Friction coefficient
θ	Angle between alpha and beta axis
$\delta_{i_{max}}$	Maximum current vector angle
ψ_f	Electromagnetic flux
δ	Torque angle

Chapter 1

Introduction

1.1 Motivation

A Traction Control System is a safety feature that has been around for a few decades in on-road use applications. It prevents vehicles from losing traction and potentially crashing if too much throttle is applied when accelerating or avoiding an obstacle, especially in wet and icy conditions when there's less traction between the tires and the road. In racing applications, a traction control aims to improve tire grip, enhancing the vehicle's straight-line and lateral acceleration, therefore improving the prototype's overall performance [1]. There are several types of traction control systems at present that work by limiting the torque from the motor to the wheels in different methods or by applying a brake force to one or more tires.

Within the area of Electronic Engineering, this dissertation will focus on building an effective and efficient motor controller that could be later applied within a traction control system for an electric motor formula student prototype vehicle, with the aim of competing at an international level, focusing not only on the dynamic performance of the prototype but bearing in mind its designs, costs of manufacturing and its overall presentation. There will be given insight into all constituting parts of a Traction Control System and the possible control methods to be utilized.

For years, motorsport has been the backbone of innovation for the automotive industry. The passion for speed provides this highly transferable innovation skills and knowledge to the automotive and other industries. In the case of a traction control system, was born as a completely mechanical system in the form of a limited-slip differential on high-power and high-torque applications, with the increase in technology, it is now complemented by electronics. Improving the traction in a fast racing car can give insight, to road car developers, on how to ensure that commercial vehicles can accelerate safely, in all weather conditions, reducing accident numbers and increasing the overall stability of a vehicle [2].

Electric vehicles have just recently become a viable option when compared to the practicality of internal combustion engine vehicles. Due to the rise of emissions and the development of battery technology, they began to emerge as low-emissions solutions. With this dissertation, the

aim is to develop a motor controller for a traction control system that could have a lasting positive impact on road use applications by boosting efficiency and safety.

1.2   Objectives

The primary objective of this dissertation is to comprehend the fundamental aspects of traction and the factors influencing it. By examining the constituting parts of a traction control system and exploring different control methods, we aim to develop an innovative and robust solution tailored specifically to the electric engine Formula Student prototype, focusing on developing an effective motor control unit.

To achieve this objective, simulation tools such as MATLAB and Simulink will be used. These powerful platforms allow us to model and simulate different traction control strategies, providing valuable insights into their performance under different scenarios. The simulations will serve as a foundation for optimizing the control algorithm, fine-tuning its parameters, and evaluating its impact on the vehicle's dynamics.

Furthermore, the dissertation emphasizes the importance of designing a reliable and efficient motor control system. As the traction control system relies on controlling the torque output to the wheels, an optimized motor control strategy is crucial for achieving the desired traction performance. Therefore, a significant portion of the research will be dedicated to developing a motor control system that integrates seamlessly with the traction control algorithm, ensuring a synergistic and harmonized operation.

By addressing these objectives, this dissertation seeks to contribute to the advancement of traction control systems for electric engine vehicles, ultimately leading to safer, more efficient, and high-performing road use applications. Additionally, the insights gained from this research can be transferred to commercial vehicles, offering valuable knowledge to developers in enhancing acceleration safety and overall vehicle stability.

In the upcoming sections, we will delve deeper into the simulation methodologies employed, detailing the design considerations for the motor control system, and showcasing the implementation and evaluation of the traction control system on the electric Formula Student prototype.

Chapter 2

State of the Art

2.1 Formula Student

Formula Student is a worldwide competition done by universities, held in the United Kingdom every year, in which students within different engineering areas come together to theorize about all the different components necessary to build a formula type car, design the prototype, manufacture the model, test everything they have created and continuously improve their project [3]. This competition allows undergraduates to apply their theoretical knowledge from a more practical perspective, enhancing their engineering skills and encouraging teamwork and project management abilities.

2.1.1 The Formula Student Vehicle

It comprises three different vehicle categories that can be designed, the Internal Combustion Engine Vehicle (CV), the Electric Engine Vehicle (EV), and the Autonomous Vehicle (AV). Each of them competes in their own class. Within these categories, the vehicles can be of physical appearance, the Formula Student Class, or the study of the project on paper, the Concept Class, to allow the progression of learning for everyone [3].

2.1.2 The Competition

During the competition, the prototype is assessed in a range of static and dynamic events by juries in distinctive fields of knowledge. Figure 2.1, bellow, explains the criteria utilized in each event and the maximum points that can be attributed to the prototypes in all classes [3].
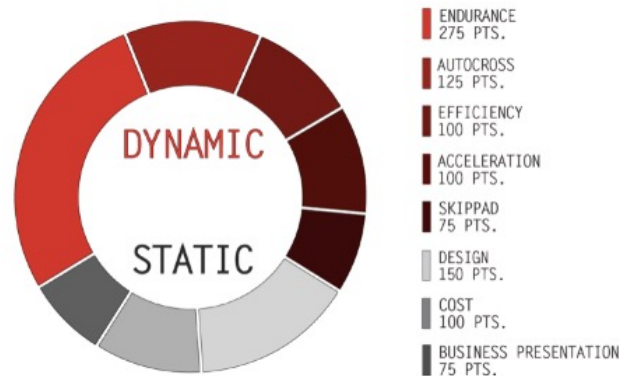
Figure 2.1: Competition Evaluation Criteria

The Static Events involve the Formula Student team explaining a series of aspects regarding the construction of the prototype or its concept, it includes:

- A business presentation, in which the image and the concept of the vehicle are sold to potential investors

- The engineering design event, that focuses on the technical aspects and the engineering process that went into developing the prototype and its software algorithms

- The cost and manufacturing event, which assesses the team thought behind the vehicles manufacturing process and the costs associated with every detail of its construction [4].

The Dynamic events comprise the overall performance of the prototype, including the vehicle's overall acceleration, in a short drag race, its lateral acceleration, within a skid pad, the time required to complete a lap, in an autocross test, and its endurance and efficiency through a long race over several kilometers [3].

When developing a Formula Student prototype, it is fundamental to understand the criteria the car will be assessed to maximize its efficiency in the event. Within the development of a traction control system, the costs, manufacturing, and overall engineering design need to be addressed throughout its process, but it is important to comprehend the tests involved in the dynamic events before commencing its development. [4] describes in detail the rules of the competition and a summary of the key areas for this project is explained below.

The Skidpad aims to measure lateral acceleration and speed on a flat surface within a constant radius of rotation. Figure 2.2 [4] shows the track layout, consisting of two circles forming an eight pattern. During the test, the vehicle will start on the starting line, it will take two full laps on the right circle, immediately followed by two full laps on the left circle, the last two laps on each side are timed and will give the final event result.
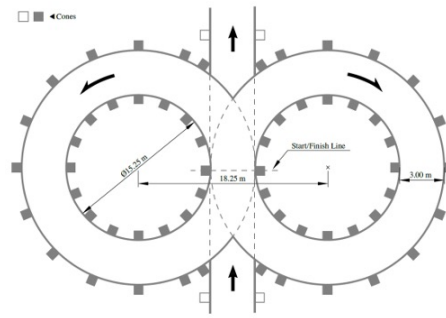
Figure 2.2: Skidpad Track Layout

The Acceleration test measures the prototype's acceleration in a straight line, on a flat surface, over a 75-meter distance. Two drivers need to attempt this test and they both have two runs.

The Autocross assesses the overall maneuverability of the vehicle within a minimum of 1.5 kilometers of track, combining acceleration, braking, and cornering performance testing in one event. The track consists of straight lines, no longer than 80m, constant turns, hairpin turns, slaloms, and chicanes, each team can attempt the course four times, two with each driver.

The Endurance and Efficiency tests aims to evaluate the overall performance of the formula student prototype, through a 22-kilometer race, on a track with similar characteristics to the autocross event. There is only one round for each team, both drivers will run for 11 kilometers each and then swap, the car is required to start and stop under its own power and no repairs are allowed during the competition. The efficiency is assessed after the endurance part of the event, as it is based on the amount of energy consumed, the mass of CO2 released to the atmosphere, and the lap times, it can be calculated as followed:

$$Efficiency\ Score = 100\ x\ \frac{(Efficiency\ Factor_{min}\ /Efficiency\ factorteam) - 1}{(Efficiency\ Facor_{min}\ /Efficiency\ Factor_{max})\ - 1} \quad (2.1)$$

Where,

$$Efficiency\ Factor = \frac{(T_min\ /LapTotalT_{min})}{(Tteam\ /Laps_{team})}\ x\ \frac{(CO2_{min}\ /LapTotalCO2_{min})}{(CO2team\ /Laps_{team})} \quad (2.2)$$

Regarding the electric vehicle itself, document [4] lists the rules required to follow for the development and construction of the prototype, some of them are listed beneath:

- Motor: only electric motors, but no restriction regarding the type of motors within this motor category, they must be connected to the accumulator through a motor controller and there is no restraint to the number of motors used

- Power limitations: for four-wheel drive vehicles, the traction system (TS) power must not exceed +60kW, regenerating energy is allowed and unrestricted and it is not allowed to supply power to the motor in a way that the car can be driven in reverse

- Brake System Plausibility Device (BSPD): regeneration is only possible when $\geq 5kW$ of power is being delivered to the motor

- Tractive System: the maximum allowed voltage between any two electrical connections is 600VDC and motor controllers/ inverters 630VDC, fans with more than 50W must not be connected

- Cells: all are accepted, except molten salt and thermal batteries

- Tractive System Energy Storage: all the cells used must be kept within a Tractive System Accumulator Container (TSAC) and this cannot surpass a maximum of 120VDC, 6MJ, and 12kg

2.2   Vehicle

As the number of vehicles in circulation increase it is important to develop this sector to the population and environmental needs. The prices of labor, materials, gasoline, petrol, and gas have been exponentially rising, becoming a big expense for car owners, and pollution levels have dramatically amplified in the past years.

The author within [5] states that to aid these issues created by traditional vehicles, governments within developed countries commenced encouraging people to purchase electric vehicles, creating supporting initiatives to assist their acquisition, including purchase discounts, tax benefits, cheaper parking, and reduced motorway fees. This solution both benefits the population - as some of their costs associated with the car are reduced; and the environment - by decreasing the high concentration of CO2 and other greenhouse pollutants.

2.2.1   Electric Vehicle

Electric vehicles have been in constant development for a few years in order to continue improving their advantages but also creating measures to deal with their challenges. Some of the general advantages described by [5] of these vehicles in comparison to traditional cars as:

- Lower CO2 and other greenhouse gases emissions

- Simpler architecture with cheaper maintenance, as they don't require as many elements as combustion vehicles

- Reliability due to simpler components design and less deterioration produced by vibrations and fuel corrosion

- Cost of electricity is lower than fuel

- Increase comfort due to fewer vibrations and motor noise

- Accessibility to all traffic areas, such as low-emission zones within big cities

On the other hand, [5] refers that the biggest challenges these vehicles currently face include:

- The driving range is short, only allowing a mean of 200 to 350km, although it has improved in the past years it still makes it hard to do long trips

- Charging time is long compared to putting fuel in the petrol station, normal charging can take up to 8h and the fast charge option takes up to 30min for 80% capacity only

- Battery packs are expensive and their manufacturing has a large carbon footprint

- Battery is large and heavy considering the vehicle's overall dimensions, weighing up to 200kg, depending on the car

Within the Formula Student competition, the electric component of the vehicle has its benefits for the traction control system for a race aim, which [2] include:

- Low emissions

- Simpler architecture and fewer components

- Possibility to create energy regeneration within the braking system

- Quick torque response of around a few milliseconds, creating a fast feedback control, compared with the combustion engines of 100-500 milliseconds

- Accurate measure of motor torque from the current, in contrast with traditional engines that has difficulties with this procedure

- Independent wheel control offers the possibility of developing in-wheel motor technologies, improving its overall stability

2.2.2 Electric Vehicles Architecture

The electric vehicle can be composed in different ways, but to optimize the performance its core configuration revolves around three subsystems: an electric motor propulsion, energy source, and auxiliary system. Figure 2.3, below, shows a general configuration model of an electric vehicle, referenced within [5].
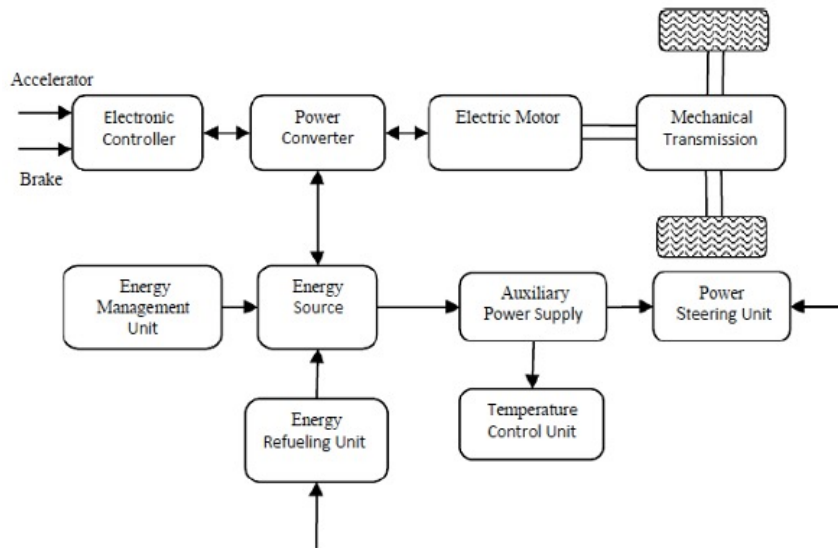
Figure 2.3: General Configuration of an Electric Vehicle

The electric propulsion system consists of converting the energy from the previous system, into power, to make the vehicle run through a chain of reactions within the drive train, involving the Electric controller, power converter, electric motor, mechanical transmission, and the driving wheels. This system also provides regenerative energy from the braking system over to the energy source. The different components of this system will be looked into, in further detail, throughout this chapter.

The energy source system provides energy to both the propulsion and auxiliary systems, it comprises the energy source, the management unit, and the energy recovery system. Batteries are the main source of energy for an electric vehicle, being lead-acid and lithium-ion the main choice for most applications. The energy management unit works hand in hand with the electronic controller and the energy recovery system to understand how much regenerative energy is being created by the braking system and if it will go to the batteries, to monitor the usability of the energy source. The energy recovery system refers to the way the energy source is charged, involving the charge port, the converters of AC supply generated by the power grid to DC required by the batteries, and monitoring parameters of this process, such as the voltage, current and temperatures reached while charging [6].

Finally, the auxiliary subsystem is responsible for supplying power to the other supporting components of the vehicle, particularly, the temperature control unit and the power steering unit. Temperature regulation is fundamental for safe operation to ensure temperature ranges and limits are followed for all the sections of the vehicle. The power steering unit is a system created to reduce the effort required to steer the car and turn the front wheels, particularly when at lower speeds while parking or maneuvering the vehicle [6].

2.2.3 Dynamic Module

Traction is defined as the resistance between the tire and the ground, without it, a car would not be able to move forward. Several variables can influence it, in the case of a Formula Student car, there is the overall weight, engine power, and the properties of the tires which play a big role in providing the needed traction. Although all these variables are important to quantify the amount of traction a car has, the traction control system will essentially use the wheel speed which will be needed to calculate the slip ratio.

To understand the limitations of the tires, Slip Ratio is defined as a dimensionless value obtained by the difference between the angular velocity of the deformed tire caused by torque being applied and the angular velocity of a free-rolling tire not subjected to any torque, to which is divided by the angular velocity of the free-rolling tire, as shown below [1].

$$Slip\ ratio = \frac{\omega - \omega_0}{\omega_0} = \frac{r * \omega - v_x}{v_x} \tag{2.3}$$

where
$\omega = Angular\ velocity\ of\ driven\ wheel\ [rad/s],$
$\omega_0 = Angular\ velocity\ of\ free\ rolling\ wheel\ [rad/s],$
$r = Radius\ of\ wheel\ [m],\quad v_x = Velocity\ of\ car\ [m/s]$

To maintain traction, a car tire must withstand forces from various axes. When accelerating, power is delivered from the motor to the tires causing a longitudinal force on the ground. This longitudinal force varies with the amount of tire slippage, i.e. varies as a function of its slip ratio and its maximum value, where the slip ratio is not at its highest value, the traction control system should adjust torque from the motors to maintain that slip ratio. This can be seen in the figure below [1].
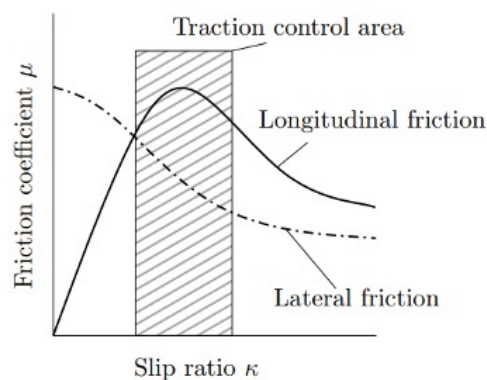

Figure 2.4: Typical tyre Behaviour

Figure 2.4 represents a typical tire behavior and shows the Slip ratio k as a function of the Friction coefficient μ. We can see that the longitudinal friction increases until the optimal equilibrium point and afterward, with a higher slip ratio, begin to decrease as stated above. Figure 2.4

also allows us to understand where the traction control system should operate, aiming to maintain the equilibrium between these two variables and maximize the longitudinal force meaning that we want to maximize the acceleration of the car having as little tire slip as possible.

At the moment of this writing, the FEUP Formula Student car is still being developed and a lot of considerations are taken into account so there is no definitive value or information regarding these variables.

2.3   Electric Motors

Electric motors convert electrical energy into rotational mechanical energy. This conversion relies on the forces generated by a magnetic field, which in turn is affected by current in the windings [7]. A magnetic field can be created by providing current to windings placed on a magnetic core, which is made of magnetic domains that point in random directions. When current starts to flow through the wire and forces the magnetic domains to line up in the direction of the current flow. All these magnetic domains pointing in the same direction means that there will be a north pole at one end and a south pole on the other, thus creating a magnetic field [8].
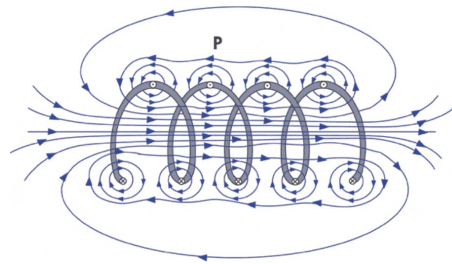
Figure 2.5: Magnetic Field Lines

Represented in 2.5 [9], is an Electromagnet, its functionality is similar to a permanent magnet as it also contains a magnetic field when current is present, but it delivers a very important feature, the ability to turn it on or off, which is not possible with a permanent magnet. If the orientation of the battery is inverted, the flow of current reverses causing the poles on the created magnet to switch places. The north pole will become the south pole and the south will become the north. This is called reversing the polarity of an electromagnet.

By placing an electromagnet in an axis near a permanent magnet, and repeatedly reversing its polarity, the attracting and repelling forces resultant of the near placing poles force the electromagnet and its axis to turn. If another permanent magnet is placed 180º from the first there will be a second force acting on the electromagnet making it spin even harder [8].

This is the basic principle of the inner workings of an electric motor. As always things evolve and nowadays exist several variants, each other with advantages and disadvantages related to efficiency, reliability, complexity, size, weight, and price as well as the more technical aspects like the voltage, current, and torque.

These aspects play an important role when choosing the most adequate motor for each application, in the case of an electric vehicle it is imperative to have high efficiency and reliability. All the other aspects are of less importance, nevertheless, require adequate attention. If the application requires a mass production vehicle accessible to everyone, the price and complexity of the motor also deserve a higher consideration, or in the case of a performance-oriented application it would be beneficial to choose a motor with high torque response, high instant power delivery and low weigh in order to keep an overall low vehicle weight.

This is the case for a PMSM which is able to achieve high efficiency and high power density, meaning that it is smaller in size for a specific power output compared with others. Its disadvantages are covered by good control techniques. Although it has less reliability than an induction motor, it delivers very good performance in several aspects. For these reasons, it will be the chosen motor to further develop this traction control system.

2.3.1 Permanent Magnet Synchronous Motors (PMSM)

A synchronous motor has the ability to produce power directly from an alternating current power source without the need for conversion being very simple and effective to control its voltage and power flow. The generator speed is directly proportional to the frequency of the generated power so it must be maintained constant at synchronous speed [10]. It is composed of a stator similar to the stator of an induction motor with three-phase windings that when connected to a three-phase power supply generate a rotating magnetic field with synchronous speed. The rotor, for small motors, is a permanent magnet opposed to the electrical magnet excited by an external DC source for larger motors.

The synchronous speed is constant and is given by the electrical frequency of the alternating current and by the number of poles in the rotor, so more coils in the stator and rotor have inferior speeds but more mechanical torque.

These features make the motors unable to accelerate or decelerate, as well as the inability to withstand significant motor loads, thus if the motor is in motion and it is accelerated or braked by external forces, the two magnetic fields fall out of synchronization causing the rotor to stop. The problems above are well mitigated by the improvements in electronics, with inverters capable of altering the frequency and power supply voltage.

A PMSM delivers very high efficiency with the ability to operate in different speed ranges without the need for a gear system. It is also very compact construction-wise compared to others, creating the possibility to be used in an in-wheel configuration. Together with the constructive similarities to an alternator, it is able to function as one, being capable of delivering power to the driving wheels and generating power in the regenerative braking phase, for this reasons coupled with the high-efficiency aspect, it is a very suitable option when considering them for an electric vehicle.

2.4   Three-Phase Power Representations

2.4.1   a-b-c Reference Frame

The a-b-c reference frame is the main way to represent three-phase power, voltage, and current, being used to model the behavior of a balanced three-phase system. It is also useful in the analysis of electric motors. Three-phase currents are often generated by a three-phase power supply. Generally, in a motor, the coils are physically placed 120º apart in the stator with designated terminals a-a', b-b', and c-c'. The induced voltages shown in Figure 2.6 [11], are called balanced phase voltages because they are out of phase 120º following the same geometry of the coils and are equal in magnitude [8].
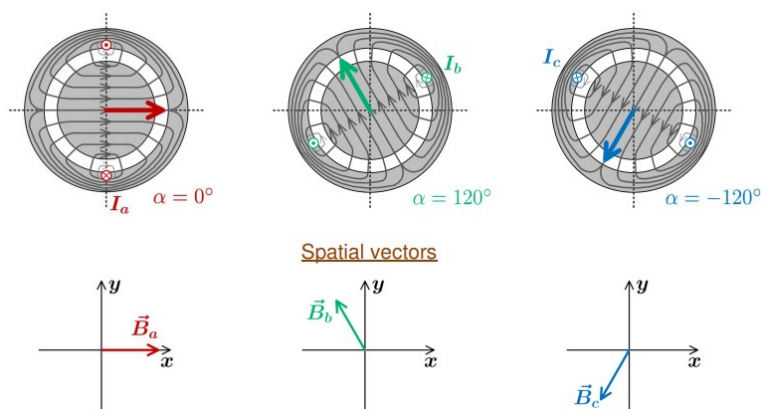
Figure 2.6: a-b-c phase sequence

A harmonic rotating movement can be described by a sinusoidal wave, thus every point in a sinusoidal wave can be tracked to a rotating spatial vector. The coil current from the three phases contained in the stator, seen in Figure 2.7, create magnetic fields on each phase-oriented depending on the order in which the currents reach their maxima [11]. The resultant magnetic field given by the sum of the three-phase magnetic fields can be seen in 2.7 [11] and is directly related to the current in each phase. The electric current flows from one phase to another which is phased 120º apart, resulting in a rotating magnetic field.
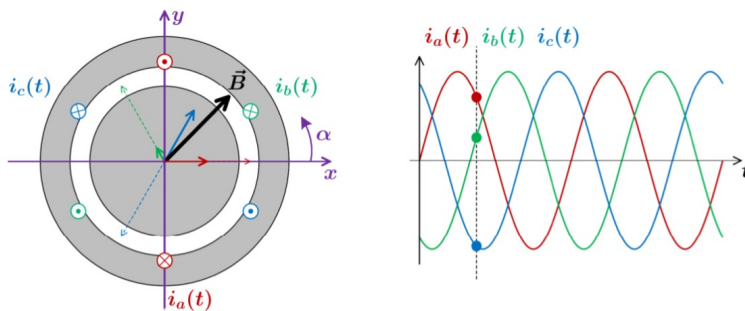
Figure 2.7: Electric currents in a Rotating Magnetic Field

The sum of an instantaneous electric current in each phase given by 2.4, compose a current space vector $\bar{i}$ shown in Figure 2.8 [12].

$$i_a + i_b + i_c = 0 \tag{2.4}$$
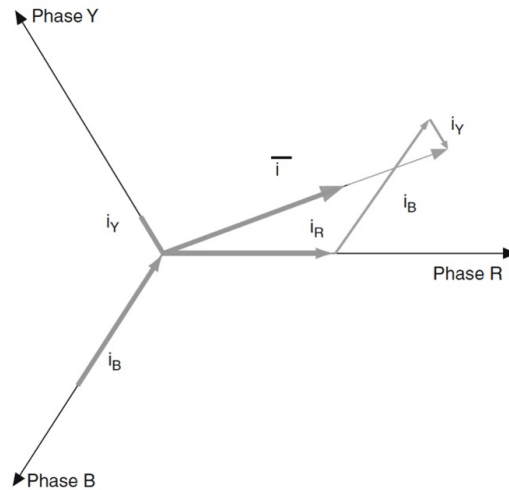
Figure 2.8: Current space vector

Where i_R, i_Y, i_B is i_a, i_b, i_c respectively and phases R, Y and B correspond to phases a, b and c.

Although it is the most directly correlated representation to the actual three-phase system, the a-b-c reference frame, always needs three components to represent any given phasor and uses complex analytical mathematical equations for control with the downside of tuning complexity and an elevated cost in some cases for the high-resolution encoder.

2.4.2 Clarke Transform

The Clark Transform is a mathematical method that is used to convert three-phase electrical quantities from the a-b-c reference frame mentioned in 2.4.1 into a two-phase system named the alpha-beta reference frame. It is the basic principle used in single-phase motors and it is widely used in the analysis and control of three-phase systems with high-performance architectures [13], as well as in the control of electric motors and other three-phase electrical devices, particularly in systems that do not contain sinusoidal waveforms, because it allows for the isolation of the fundamental and harmonic components of the waveform.

At any given moment, a space vector only needs two variables to be defined, so the current space vector seen in Figure 2.8, can be simplified using a two-axis theory. The current vector will be defined by a real segment equal to the instantaneous value of the direct-axis current component i_α and by an imaginary segment equal to the quadrature-axis current component i_β, a graphic representation can be seen in Figure 2.9 [12].
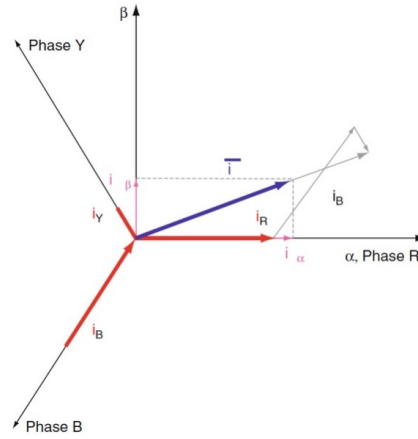
Figure 2.9: Current space vector in the $\alpha\beta$ frame

Once again the nomenclature in figure 2.9 of R, Y and B relates to the nomenclature in this paper as a, b and c respectively. The current vector is then expressed as equation 2.5:

$$\bar{i} = (i_\alpha + i_\beta) \tag{2.5}$$

This α and β current components are fictitious two-phase values, so they need to be related to its three-phase components [12], which is done in a matrix form by use of equation 2.6.

$$\begin{bmatrix} i_\alpha \\ i_\beta \end{bmatrix} = k * \begin{bmatrix} 1 & -\frac{1}{2} & -\frac{1}{2} \\ 0 & \frac{\sqrt{3}}{2} & -\frac{\sqrt{3}}{2} \end{bmatrix} * \begin{bmatrix} i_a \\ i_b \\ i_c \end{bmatrix} \tag{2.6}$$

For an amplitude invariant transformation, the value of k should be $k = \frac{2}{3}$ and for a power invariant transformation, $k = \sqrt{\frac{2}{3}}$ [12]

In this paper it will be used the power invariant constant, so the Clarke Transformation used to transform a three-phase system (a, b, c) to a two-phase system (α, β) is defined in equation 2.7 [12].

$$\begin{bmatrix} i_\alpha \\ i_\beta \end{bmatrix} = \sqrt{\frac{2}{3}} * \begin{bmatrix} 1 & -\frac{1}{2} & -\frac{1}{2} \\ 0 & \frac{\sqrt{3}}{2} & -\frac{\sqrt{3}}{2} \end{bmatrix} * \begin{bmatrix} i_a \\ i_b \\ i_c \end{bmatrix} \tag{2.7}$$

The major advantage of using the Clark Transform is that it allows for the analysis and control of three-phase systems in a simpler two-dimensional space, which can be more convenient, easier to understand, and to control.

The original values can be obtained through the inverse Clarke Transform seen in 2.8.

$$\begin{bmatrix} i_a \\ i_b \\ i_c \end{bmatrix} = \frac{1}{k} * \begin{bmatrix} \frac{2}{3} & 0 \\ -\frac{1}{2} & \frac{\sqrt{3}}{2} \\ -\frac{1}{2} & -\frac{\sqrt{3}}{2} \end{bmatrix} * \begin{bmatrix} i_\alpha \\ i_\beta \end{bmatrix} \tag{2.8}$$

By replacing k in equation 2.8, equation 2.9 is obtained.

$$\begin{bmatrix} i_a \\ i_b \\ i_c \end{bmatrix} = \frac{3\sqrt{2}}{2} * \begin{bmatrix} \frac{2}{3} & 0 \\ -\frac{1}{2} & \frac{\sqrt{3}}{2} \\ -\frac{1}{2} & -\frac{\sqrt{3}}{2} \end{bmatrix} * \begin{bmatrix} i_\alpha \\ i_\beta \end{bmatrix} \tag{2.9}$$

2.4.3   Park Transform

The Park Transform performs in a similar fashion as the Clarke Transform, in a sense that relates one reference frame to another, only in this case the base reference to be transformed is the Clarke Transform. The aim is to go from a stationary reference frame $\alpha\beta$ to a rotating reference frame known as dq, 2.10 [12], which stands for direct and quadrature components and relate to the alpha-beta frame by the angle between the two frames. The dq frame will now rotate at the speed of the rotor at synchronous speed, therefor our space vector will be static from the point of view of this new rotating reference frame [12].
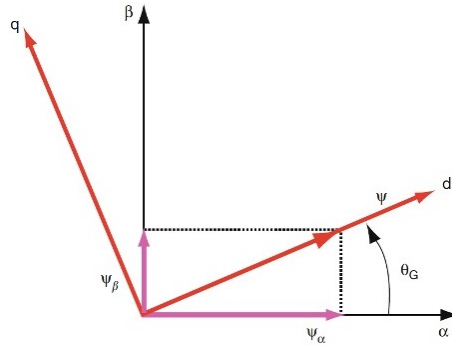
Figure 2.10: Rotating frame of reference d-q

Mathematically, the Park Transform and the Inverse Park Transform are given respectively by equation 2.10 and equation 2.11 [12].

$$\begin{bmatrix} d \\ q \end{bmatrix} = \begin{bmatrix} \cos(\theta) & \sin(\theta) \\ -\sin(\theta) & \cos(\theta) \end{bmatrix} * \begin{bmatrix} \alpha \\ \beta \end{bmatrix} \tag{2.10}$$

$$\begin{bmatrix} \alpha \\ \beta \end{bmatrix} = \begin{bmatrix} \cos(\theta) & -\sin(\theta) \\ \sin(\theta) & \cos(\theta) \end{bmatrix} * \begin{bmatrix} d \\ q \end{bmatrix} \tag{2.11}$$

Where θ is the angle between (α, β) and (d, q)

In the a-b-c frame, three sinusoidal references for each phase need to be tracked. In the alpha-beta frame, only two sinusoidal references for each orthogonal component need to be tracked,

but in the dq frame, a constant DC reference is tracked which is easily done by common simple controllers and it is possible to use directly Space Vector Modulation (SVM).

Consecutively implementing these two transforms and converting AC voltage and current components into DC signals, greatly simplifies computation and it is easier to control.

2.5 Power Converters

An converter is an electronic device that converts DC voltages and currents to AC waveforms[11]. It also can function in the reverse way, converting AC to DC. From one or more DC sources, it transforms the input current into alternating current with the ability to adjust frequency, phase, and amplitude to best fit a particular application. The basic principle behind the operation of a converter is shown in Figure 2.11 [11]. In electric vehicles, converters are used to convert the DC electricity stored in the battery pack into alternating current, which is used to power the electric motor or motors. The converter is a key component of the EV powertrain and plays a critical role in the development of the control system. This conversion is accomplished by the proper modulation of the power switches that compose the converter. The switches topology provides different configurations and conducting states.
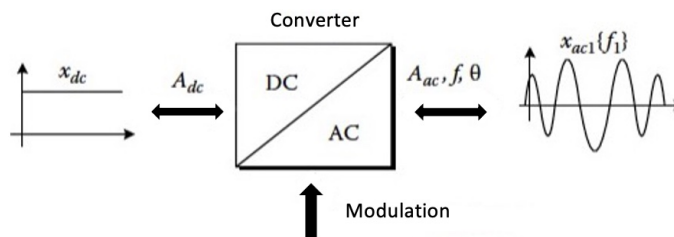
Figure 2.11: Converter Operating Principle

Converters can be divided into two primary groups. The current source converter (CSC) with a current source as the name implies, and the voltage source converter (VSC) with a voltage source.

2.5.1 Voltage Source Converters

VSC are the most usual power conversion systems in DC-AC applications. They draw constant voltage from a capacitive DC link and a voltage source rectifier. The output is a switched voltage waveform with variable phase, frequency, and amplitude matching to a required reference voltage. The output current is usually sinusoidal for inductive loads like motor drives and is defined by the load [11].

The half-bridge is one of the most important topologies in power systems because it is the base principle to then construct a three-phase converter. It is a two-level single-phase converter containing two transistor switches such as IGBTs (Isolated Gate Bipolar Transistors) or any other power semiconductor, this transistor pair is known as a leg. Figure 2.12 [11] shows a half-bridge

single-phase converter consisting of one leg connected to a DC link. The DC link is there to split the voltage from the power source and provide a zero volt midpoint to connect the load [11]. This midpoint is known (node o in Figure 2.12) as the neutral point and the load is connected between this point and node a which is the converter leg output point.
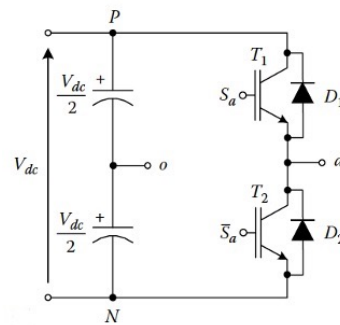
Figure 2.12: Half-bridge converter power circuit featuring IGBTs

This type of converter, being a two-level, means there are only two possible output voltages. Switching between the two possible states over a period of time is what's called modulation. The two possible states are achieved by controlling a binary gate signal (S_a in Figure 2.12). When S_a is equal to 1, T1 is ON (conducting, meaning that the output node a is connected to P, producing a positive output voltage) and T2 is OFF. If S_a is equal to 0 then T1 is OFF and T2 is ON, producing a negative output voltage. With just three of these converter legs connected in parallel, a three-phase converter called a full-bridge voltage source converter is obtained. An example circuit with IGBTs and a load connected in the form of a star is displayed in Figure 2.13 [11].
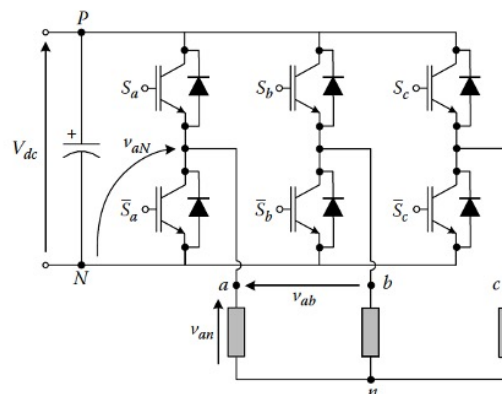
Figure 2.13: Full-Bridge Three-Phase VSC power circuit

It has the same working principles of the half-bridge converter, its modulation is also done by controlling the binary inputs, only in this case there are three of them, S_a, S_b and S_c. As with the half-bridge, the switches in each leg are implemented with complementary signals, in order to

avoid the conduction of both transistors at the same time and therefore short-circuit the DC link
[11]. This converter contains three legs, so it needs input from three binary signals. That means it
features $2^3 = 8$ distinctive switching states.

This topology has a very high voltage derivative and is not suitable for the high-power range
due to switching losses which can be mitigated by the use of special modulation techniques [11].

2.5.2   Modulation Methods

Modulation is defined as the alternation between the possible switching states in order to gen-
erate a voltage waveform. Several methods with different performances, operating principles, and
implementations will be reviewed in the following sections. The choice of a particular modulation
technique can be chosen depending on its power range or dynamic requirement in order to best fit
the desired application.

2.5.2.1   Square-Wave Modulation

Square-wave modulation thrives for being the easiest to implement as it is the most basic
modulation scheme for the VSC. The intention is to obtain from the converter an AC square output
waveform with a specific frequency [11].

The converter's output voltage waveform is represented in Figure 2.14 [11], where can be seen
that phase a is alternating between 0 and V_{dc} every half fundamental cycle. This alternation value
is obtained by simply comparing the values of the reference voltage and zero. A block diagram
of this simple control strategy can be seen in Figure 2.15 [11]. The other phases follow the same
control principle, only shifted by $2\pi/3$ rad or 120 degrees from each phase.
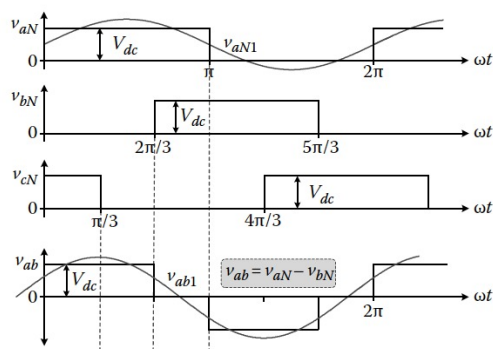
Figure 2.14: Square-Wave Operation - Voltage Waveforms
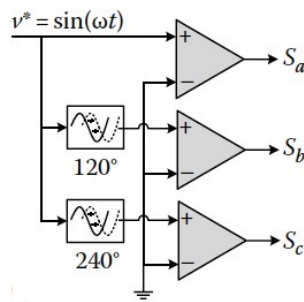
Figure 2.15: Square-Wave Operation - Block Diagram

The VSC single-phase solution has little to no practical use, even the three-phase square-wave method is obsolete by today's standards, only being used in low-dynamic performance systems and low-cost systems. As said in [11], low power quality is the price to pay for implementation simplicity and efficiency, since devices switch at the fundamental switching frequency.

2.5.2.2 Sinusoidal Pulse Width Modulation

Sinusoidal Pulse Width Modulation (PWM) is the most developed and most common modulation scheme in power converters due to its simple implementation, and good power quality. On the other hand, it needs higher switching frequencies which affects efficiency as it introduces more switching losses, which not being appropriate for high-power applications. However, with a low switching frequency, an increase in cost and size can appear for the necessary filters, so a choice has to be made between the filter design cost and the power losses.

PWMs alternate between switching states so that the average of the switched voltage waveform equals the desired reference [11]. The output voltage in the converter is fixed, and the pulses can be either fully on or fully off meaning that there are only two possible states that the pulse can be in: high (on) or low (off); so the modulation is done by altering their width, better known as the duty cycle. A representation of this variation can be seen in Figure 2.16(a) [11]. Implementation in the digital form, sample and hold the desired value through the modulation period and then computing the duty cycle by averaging the value or by comparing it to the carrier waveform. There are three different configurations inside the sinusoidal PWM, the bipolar in which the output voltage shifts from the positive and negative output voltages, the unipolar switching from zero and positive output voltages or between zero and negative and the multicarrier strategy used in multilevel converters [11]. A three-phase VSC bipolar PWM control block diagram is illustrated in Figure 2.16(b) [11].
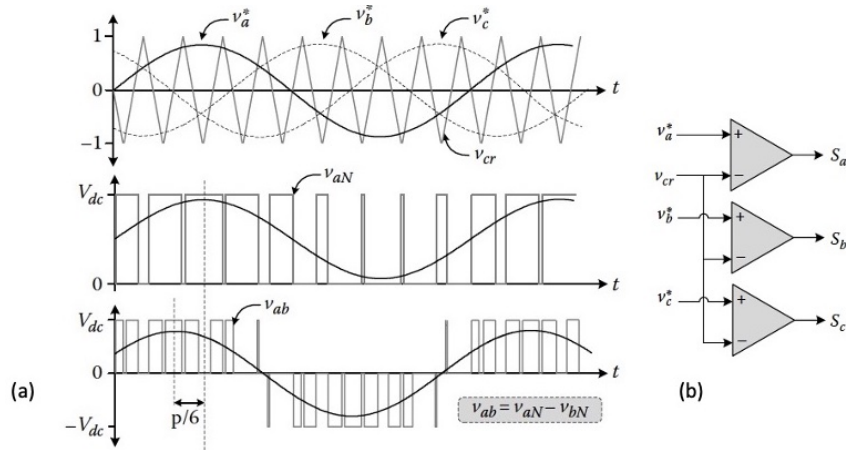
Figure 2.16: (a) - Multicarrier Configuration on top, Unipolar configuration in the middle, and Bipolar configuration on the bottom and (b) Three-Phase VSC Bipolar PWM

Unipolar PWM is often used in applications where only one polarity of the voltage is required, such as rotating a motor in one direction or controlling the intensity of an LED. Bipolar PWM is typically used in applications where both polarities of voltage are needed, for example when driving a motor in both directions.

2.5.2.3 Space Vector Modulation

Space Vector modulation (SVM) relies on the PWM strategy only differing from the switching times that are calculated based on the three-phase vector representation of the VSC switching states and its reference compared to the time representation of the phase-amplitude from previous methods. The voltage space vector is defined in the $\alpha\beta$ plane by:

$$v_s = \frac{2}{3} * [V_{aN} + aV_{bN} + a^2V_{cN}] \tag{2.12}$$

Where,

$$a = -\frac{1}{2} + j\frac{\sqrt{3}}{2} \tag{2.13}$$

and V_{an}, V_{bn}, V_{cn} are the phase output voltages from the converter. The previous equation can be written in terms of all binary combinations to obtain equation 2.14, leading to eight space vectors, with only seven different of them because vectors 0 and 7 produce the same voltage level which is zero. Figure 2.17 [11] shows the space vectors as well as the operating principle for a generic sector.

$$v_s = \frac{2}{3} * V_{dc}[S_a + aS_b + a^2S_c] \tag{2.14}$$
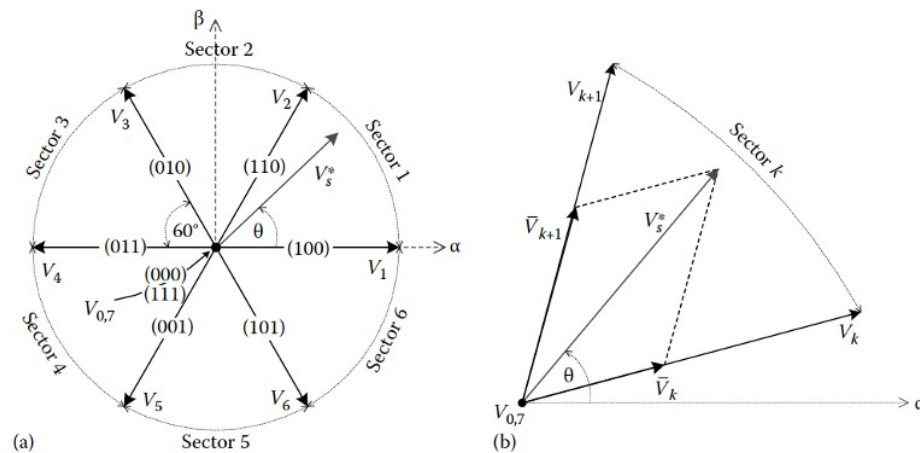
Figure 2.17: (a) Space Vectors generated by a three-phase VSC and (b) SVM operating principle for a generic sector k

Space Vector modulation is more efficient than the other studied methods as it allows for smoother control of the motor and higher resolution of the PWM signal.

Its main advantages are:

- Improved efficiency: SVM generates signals that result in a more efficient operation, producing a more continuous flow of current. This results in fewer losses and therefore more efficiency

- Higher resolution: It allows for a higher resolution of the signal and leads to a motor with improved controllability and accuracy. This provides a smoother operation and better response to control inputs

- Reduced harmonic content: SVM produces less harmonic noise which can lead to lower electromagnetic interference and better power quality

- Increased bandwidth: wider bandwidth means faster response of the motor to control inputs, being quite useful in applications where fast response times are needed, such as in servo systems

2.6 Control Methods

There are two main control methods for induction motors: scalar and vector control. Scalar control only adjusts the magnitude and frequency of the components, while vector control also adjusts their instantaneous positions. Scalar control is typically used in low-performance, open-loop systems and is based on steady-state relations. In contrast, vector control is used in dynamic states and is based on the relations valid in these states. It adjusts the positions of the space vectors to maintain their correct orientation during steady states and transients, which allows it

to dynamically decouple electromagnetic flux and torque. As a result, vector control belongs to high-performance control and is implemented in a closed-loop fashion. Vector control can be implemented in many ways but the most prominent ones are Field-Oriented Control (FOC), Direct Torque Control (DTC), and DTC with Space Vector Modulation (DTC-SVM). Since Scalar Control is more suitable for low-performance applications, the focus will be on Vector Control techniques.

2.6.1 Field-Oriented Control

Field-Oriented Control (FOC) is a control method used in electric motor drives to improve their performance and efficiency. It is particularly useful for controlling the torque and speed of AC induction motors and permanent magnet synchronous motors.

Before vector control methods became popular, motors were controlled using simpler control schemes that usually relied on open-loop control techniques. For example, in Voltage Control, the motor's speed and torque are controlled by directly adjusting the voltage applied to the motor's stator. By increasing or decreasing the voltage level, the motor's speed can be adjusted. However, this can result in poor performance and low efficiency, especially at high speeds. FOC addresses this issue by decoupling the control of the torque and the flux in the motor.

To implement FOC, the stator currents of the motor are first transformed into a rotating coordinate system that is aligned with the rotor flux. The transformed stator currents are then decomposed into two components: the d-axis current, which is responsible for controlling the flux, and the q-axis current, which is responsible for controlling the torque. In the d-axis and q-axis, seen in Chapter 2.4, currents can then be independently controlled to achieve the desired torque and flux in the motor.

The FOC technique is based on the principles of a mechanically commutated DC brush motor, in which the flux and torque are independently controlled using separate exciting and armature windings. In contrast, a cage-rotor IM has a single three-phase stator winding, and the stator current vector (Is) is used for both flux and torque control, resulting in a coupling between the exciting and armature currents. This is addressed by the decoupling function mentioned above, decomposing the instantaneous stator current vector into two components. This allows the control of the IM to be implemented using a cascaded structure with linear PI controllers, similar to a separately excited DC brush motor [11]. A circuit diagram of a fundamental FOC scheme is shown in Figure 2.18 [14].

There are two main types of field-oriented control (FOC): indirect FOC and direct FOC. Both methods are used to achieve the decoupled control of torque and flux in electric motors, but they differ in how they handle the estimation or measurement of the rotor flux vector position.

In indirect FOC or sensorless FOC, the position of the rotor flux vector is not directly measured or estimated. Instead, it is calculated based on the reference values and the measured mechanical speed or position of the motor. The control system uses mathematical models and algorithms to determine the position of the rotor flux vector indirectly. Typically, a mathematical observer, such

as a sliding-mode observer, is used to estimate the rotor flux position based on the available sensor data.

In contrast, in direct FOC, the position of the rotor flux vector is either directly measured using sensors or estimated using sensor-based methods like encoder or resolver feedback. The control system has direct information about the rotor position, allowing for precise control of the flux vector. The choice between indirect and direct FOC depends on the specific requirements of the motor drive system. Indirect FOC is typically used when precise speed or position measurement is available, while direct FOC is used when a precise measurement is not possible or when the flux vector needs to be estimated [11].
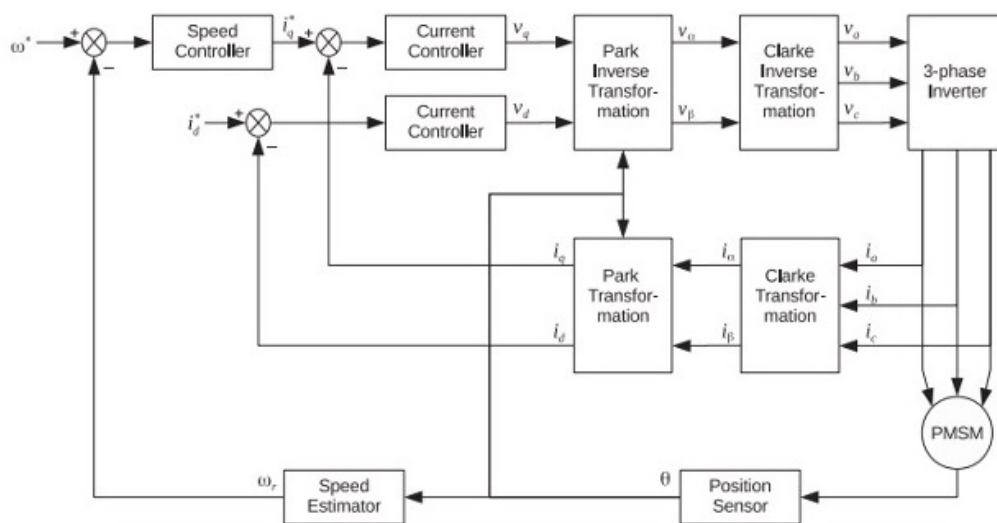
Figure 2.18: Fundamental Field-Oriented control scheme

2.6.2 Direct Torque Control

In Direct Torque Control (DTC), the torque and flux produced by the motor are directly controlled using the stator currents of the motor. The stator currents are adjusted to produce the desired torque and flux, and the stator flux and rotor position are estimated using sensors or observers. The estimated stator flux and rotor position are used to determine the reference stator currents that produce the desired torque and flux. The actual stator currents are then adjusted to match the reference stator currents, using a current control loop [11].

DTC has a few advantages over traditional control methods, such as field-oriented control (FOC), depending on the requirements and the application. It does not require a complex current transformation and decomposition process, and it can be implemented using a simple control structure which can be seen in Figure 2.19 [11]. DTC also has good dynamic performance and is capable of fast torque response. However, it requires precise sensors or observers to estimate the stator flux and rotor position, and it may have lower efficiency compared to FOC at low speeds.
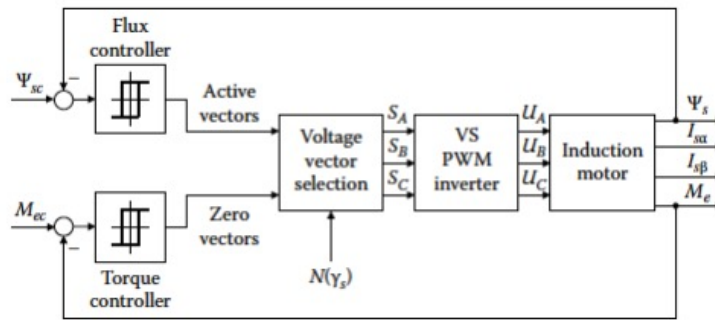
Figure 2.19: Generic block scheme of DTC

2.6.3 DTC with Space Vector Modulation

Hysteresis-based direct torque control (DTC) schemes have some disadvantages, such as a variable switching frequency, the need to follow strict rules for maintaining polarity consistency, current and torque distortion due to sector changes, difficulty with starting and low-speed operation, and the requirement for a high sampling frequency for digital implementation. When a hysteresis controller is implemented on a digital signal processor (DSP), its operation differs from that of an analog implementation. In the analog version, the torque ripple is kept within the hysteresis band and the switching instants are not equally spaced, while in the discrete version, the controller operates at a fixed sampling time and requires a fast sampling frequency to operate like the analog version. These issues can be addressed by using a closed-loop control scheme with a PI, predictive/deadbeat, or neuro-fuzzy controller to calculate the required stator voltage vector, which is then synthesized using a pulse width modulation (PWM) technique or a variation of one, such as the SVM (Space Vector Modulation) [11].

DTC-SVM is a variant of direct torque control (DTC) that uses space vector modulation (SVM) to synthesize the stator voltage vectors needed to produce the desired torque and flux in the motor.

DTC-SVM scheme displayed in Figure 2.20 [11], has several advantages over traditional DTC schemes. It does not require a hysteresis controller, which eliminates issues such as torque ripple and low-speed operation problems. It also allows for a lower sampling frequency compared to traditional DTC, which simplifies the digital implementation and reduces the computational burden. However, it requires precise sensors or observers to estimate the stator flux and rotor position, and it may have lower efficiency compared to traditional DTC at low speeds.
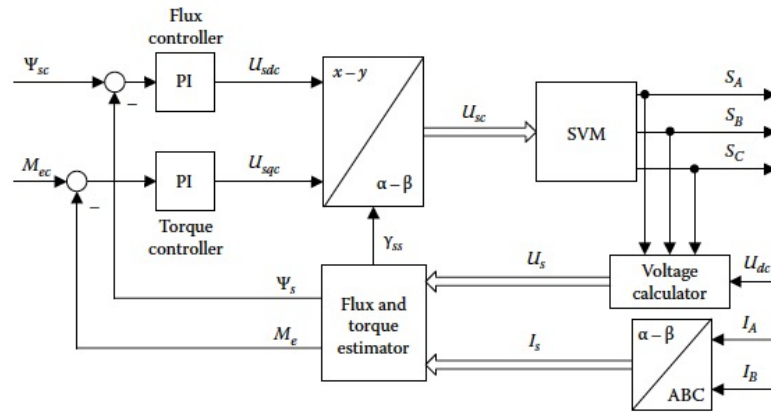
Figure 2.20: DTC-SVM scheme

For improved low-speed operation performance, it is recommended to use indirect R-FOC (Rotating-Flux-Oriented Control) with a speed/position sensor. However, this scheme is sensitive to changes in the rotor time constant, which must be adapted online. On the other hand, DTC (Direct Torque Control) has a very fast torque response, a simple structure, does not require a shaft motion sensor, and is less sensitive to changes in IM parameters compared to FOC. For sensorless operation, DTC or direct R-FOC can be used. To reduce torque ripple and fix the inverter switching frequency, SVM (Space Vector Modulation) has been introduced into the DTC and FOC structure. This combines the advantages of FOC and eliminates their disadvantages, making it an excellent solution for general-purpose IM (induction motor) and PMSM (permanent magnet synchronous motor) drives.

Chapter 3

Controller Design

Field-Oriented Control presents several advantages for controlling electrical machines, especially in applications such as motor drives, as it allows for independent control of the motor's magnetic flux and torque components. As a result of the study conducted in Chapter 2.6, the preferred choice was to use FOC. The ability to decouple the control of these two components enables very precise regulation of the motor's speed and torque values, resulting in higher dynamic response, efficiency, and performance.

The decision to adopt FOC was based on its potential to deliver superior performance, efficiency, and robustness in controlling electric motors, which aligns with the principles of this dissertation. Furthermore, this strategy proves to be a reliable control strategy as it has been widely studied and implemented throughout several pieces of research.

FOC as a vector control method, seeks to align the stator flux vector with a particular angle relative to the rotor flux vector. The selection of the optimal orientation angle between the rotor and the stator flux vectors relies on the rotor characteristics of the PMSM, one being its anisotropy. Additionally, the angle choice depends on the control strategy.

As explained in Chapter 2.6.1, the interaction between stator currents and rotor flux takes place as the interaction between stator and rotor flux. In this representation, which enables a more intuitive understanding of the association, the direct axis component of the stator current is responsible to reinforce or to reduce the rotor flux depending if it is positive or negative respectively. Whereas the quadrature axis component is primarily responsible for controlling the amount of electromagnetic torque differing from a motor operation if it is positive or a generator operation if negative. Overall, the goal is to line up the stator current with its desired direct and quadrature axes components, allowing for effective control over the performance of the motor while outputting the needed torque [15].

3.1 Control Strategy

FOC is a control method in itself, advantageous for the reasons stated above, however, it is not a specific control strategy. It delivers the foundation to accurately control the motor's current and

torque by providing a framework and a set of principles that allow the controlling of PMSMs, but
the implementation of control strategies within that framework is still needed in order to achieve
high-performance requirements [11]. Several control strategies can be employed and they differ
in how torque and flux components are managed. The main existing strategies are:

- Maximum Torque-per-Ampere Control (MTPA)

- Constant Torque-Angle Control

- Flux Weakening Control

- Maximum Efficiency Control

- Maximum Torque-per-Voltage Control

Essentially, each control strategy yields on adjusting direct and quadrature current references
(i_d^* and i_q^*) to the FOC current loop. Only Maximum Torque-per-Ampere Control and Constant
Torque-Angle Control will be addressed in this dissertation.

3.1.1   Maximum Torque-per-Ampere Control

Maximum Torque-per-Ampere (MTPA) Control focus is to, as the name suggests, maximize
the motor torque production per each unit of current, by adjusting the current vectors orientation
in such a way that boosts the torque output to its maximum for a given current magnitude [16].
Using FOC to control the direct and quadrature axes appropriately, allows the motor to operate
near its maximum torque capability with minimal copper losses. This is the most commonly used
strategy for FOC.

In Figure 3.1 can be seen the MTPA trajectory, corresponding to the tangent points in the
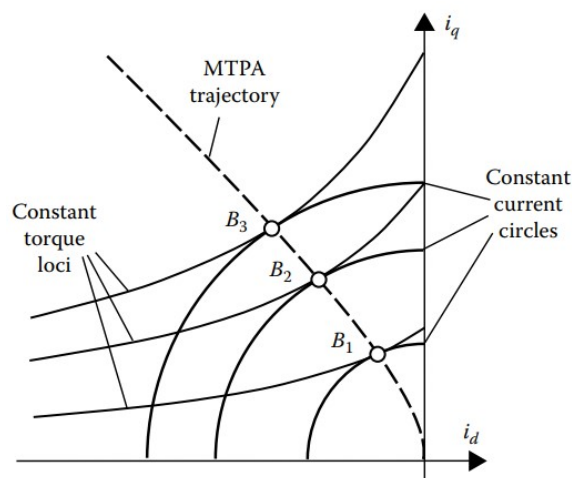constant current circles [11].

Figure 3.1: Current vector trajectory for MTPA control

Electromagnetic torque is given by [11]:

$$T_e = \frac{3}{2} P \left(\psi_f i_q + (L_d - L_q) i_d i_q \right) \tag{3.1}$$

Where:

- L_d and L_q - direct and quadrature motor inductances, retrieved from the EMRAX228 datasheet

- P - number of pole pairs

- i_d and i_q - direct and quadrature currents

The current vector angle $\delta_{i_{max}}$ provides the maximization of the torque. According to [11], it is given by:

$$\delta_{i_{max}} = cos^{-1} \frac{-\psi_f + \sqrt{\psi_f^2 + 8(L_d - L_q)^2 i_s^2}}{4(L_d - L_q) i_s} \tag{3.2}$$

And,

$$i_d = i_s cos(\delta_i) \tag{3.3}$$

$$i_q = i_s sin(\delta_i) \tag{3.4}$$

Since the implementation motor, the EMRAX 228, has very similar direct and quadrature axes inductances (which will be seen in Chapter 4.1), it can be considered to have an anisotropic rotor with L_d slightly lower than L_q and thus MTPA can be achieved with a small negative i_d current, corresponding to a flux weakening operation region.

With PMSM anisotropic rotors, the equation 3.1 becomes the same as the Constant Torque-Angle Control electromagnetic torque equation 3.6 because $L_q = L_d$. This means that the MTPA control strategy converts into the Constant Torque-Angle Control strategy [15].

3.1.2 Constant Torque-Angle Control

In Constant Torque-Angle Control, a fixed angle is maintained between the direct axis reference angle and the rotor flux vector, i.e. the torque angle δ is kept at an angle of 90 degrees. If i_s is kept at this angle from the rotor flux vector, the result is a i_d set to zero [15].

$$\theta = 90° \Rightarrow i_q = i_s sin(-\theta) = i_s \Rightarrow i_d = 0 \tag{3.5}$$

By ensuring a constant angle association, torque production can be controlled with more accuracy.

Since the direct current reference is zero, the electromagnetic torque now becomes:

$$T_e = \frac{3}{2} P \psi_f i_q \tag{3.6}$$

This equation 3.6 will be implemented in the simulation chapter. It can be seen in Figure 4.17.

Both control strategies (MTPA and Constant Torque-Angle Control) are important strategies in FOC, allowing for improved performance, enhanced control over torque production as well as efficient utilization of the PMSM characteristics. For this reason, it will be the adopted control strategies.

3.2   System Overview

The main layout of the system seen above contains the main components needed for it to run. The FOC block implements the whole control algorithm and sends the gating signals to a three-phase 2-level converter. The power conversion stage is comprised of the DC link that powers the converter which then converts the DC voltage into a three-phase AC voltage applied to the motor windings.
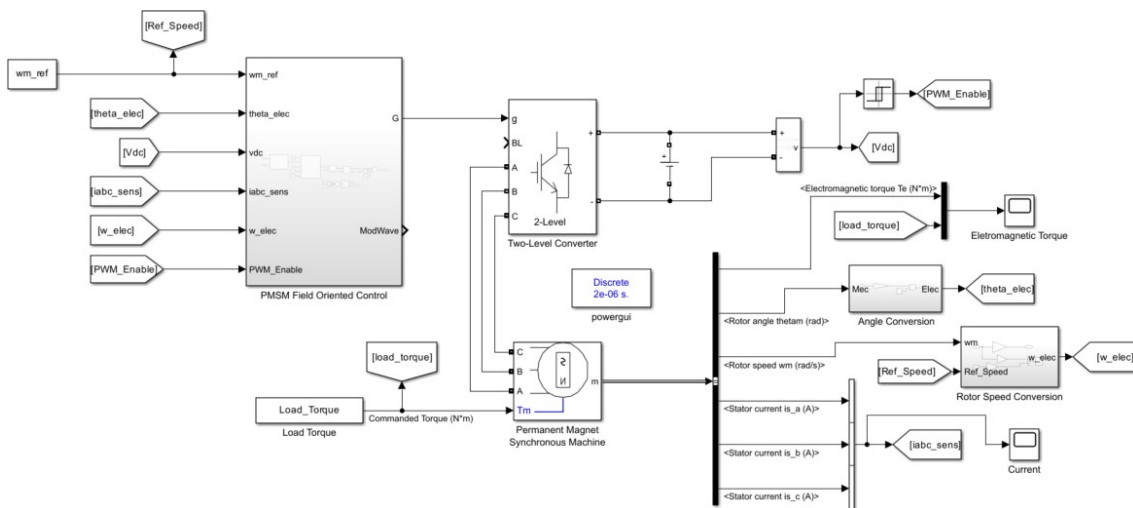
Figure 3.2: System Overview in Simulink

A few important measurements are then extracted from the motor such as Current Measurements - the knowledge of these values provides feedback to the control system that enables an accurate control of current magnitudes and phase angles; Rotor Position Detection: it is crucial to FOC to know the position of the rotor to accurately align the magnetic field of the rotor with the stator field.

Field-Oriented Control is a feedback loop control system, so the current, rotor angle and speed measurements that take place in the motor are then fed back into the control system block. The algorithm continuously receives feedback from these measurements, automatically adjusting the control signals, aiming to achieve the desired performance and accuracy. The feedback loop ensures that the motor operates as intended, comparing the measured signals to the desired reference

values. Any deviations between the two values are then used to adjust the control actions accordingly [11].

3.3   Control Algorithm

As stated above, Field-Oriented Control has been selected as the preferred approach to proceed with this dissertation. The execution algorithm is executed after the initial reference values such as torque and speed are set, with the following steps [15]:

- Measure Stator Currents: although the current measurement is done outside of this block, it is part of the algorithm and is an input of the control block. Through current sensors, the three-phase currents (i_a, i_b, and i_c) are obtained.

- Coordinate Transformation: Convert the three-phase currents (i_a, i_b, i_c) from the stationary reference frame (abc or $\alpha\beta$ axes) to the rotating reference frame (dq axes) using the Clarke and Park transforms enabling independent control of torque and flux components.

- Calculate Control Signals: Apply control algorithms to generate control signals for the voltage source inverter based on the transformed dq currents and rotor speed. Calculate the speed control signal to feed the quadrature axis current reference by computing the errors to a PI controller. Using both current references for the direct and quadrature axes, calculate the current control loop by adjusting the currents based on the deviation between the measured and reference values and computing the deviation to PI controllers.

- Pulse Width Modulation (PWM) Generation: Generate PWM with SVM signals based on the control signals obtained in the previous step. The PWM signals determine the duty cycles and timings of the voltage source inverter's switches, shaping the desired voltage waveforms to the motor.

- Repeat: Continuously repeat steps 1 to 4 in a closed-loop manner to achieve real-time control. Measure the currents, perform the coordinate transformation, calculate control signals, generate PWM signals, and update control parameters based on the feedback information.
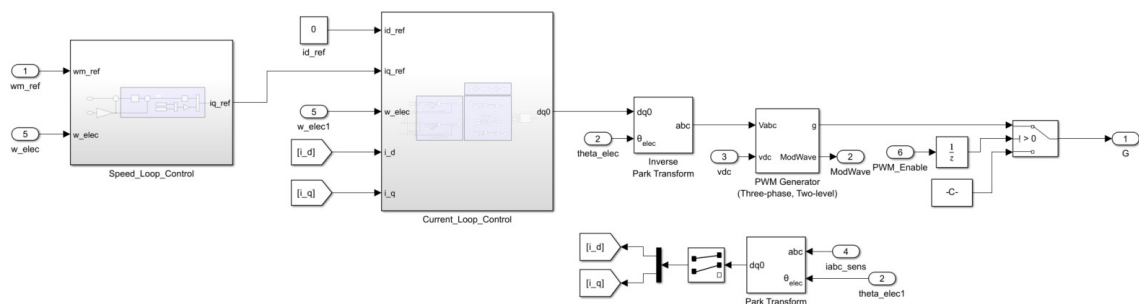
Figure 3.3: FOC Control System in Simulink

Figure 3.3 shows the schematics for the Field Oriented Control algorithm, containing a Speed Loop Control block and a Current Loop Control block that will be developed further in the following chapter. It also contains a block for the Park and the Inverse Park Transform which are a part of the Simulink Block Library as well as a PWM Generator block.

With FOC as the selected control method, the succeeding chapters will focus on the simulation and implementation of this strategy using appropriate tools and techniques. By leveraging simulation environments, such as Simulink from MATLAB. This simulation stage is vital for validating the structure and performance of the FOC algorithm and it also provides an opportunity for optimization before the actual implementation on the microcontroller unit.

Chapter 4

Modeling and Simulation

This chapter aims to implement and simulate the control algorithm and strategies. After carefully considering and selecting the control method from the previous chapter, it becomes clear the entire control algorithm should be implemented and tested prior to practical implementation. This way, through a systematic approach, is possible to validate the structure of the system and fine-tune all parameters, ensuring the reliability of the results, before attempting to implement it on the microcontroller unit.

The simulation tool used in this study was Simulink. Simulink is a powerful tool from Math-Works Inc. integrated within MATLAB that provides a comprehensive platform for modeling, simulating, and analyzing dynamic systems, making it well-suited for this purpose.

It offers a graphical block diagram environment where users can visually represent the system components and their interactions. The chosen control algorithm, along with its various components such as the motor, measurement probes, and controllers, can be modeled using Simulink blocks. These blocks can be connected to define the system's behavior and simulate its response under several user-defined parameters and conditions.

The seamless integration with MATLAB is a big advantage that allows its users to easily incorporate custom algorithms and mathematical functions, resulting in a tool that provides high flexibility when implementing control algorithms.

In summary, Simulink, integrated with MATLAB, was utilized in this chapter for the simulation of the chosen control algorithm. The graphical block diagram environment, coupled with the ability to incorporate custom algorithms and functions, facilitated the accurate modeling and analysis of the control system's behavior. This simulation step allowed for validation, fine-tuning, and optimization of the control algorithm before further implementation.

4.1 Electrical Parameters

The goal of the simulation is to validate the system prior to implementation, this allows the testing of different schematics as well as optimization of the overall system. This means it is important to have the simulation really close in terms of parameters to the actual setup.

The motor, an EMRAX 228 High Voltage, on which the simulation was based, delivers a peak motor power of 109 Kw but only briefly. The continuous power delivery is 62 Kw when working with liquid and air cooling. It is a salient pole-free machine with a smooth outer rotor configuration, contributing to its small and compact size, making it well-suited for vehicle applications, weighing only 12.9 to 13.5 kg. The motor's windings are connected in a Y (star) configuration (Appendix A). This type of winding connection allows the motor to achieve maximum torque output for its power rating, indicating an efficient utilization of power, being capable of reaching up to 96% of efficiency.

Additionally, the motor incorporates a resolver to measure the rotor position as well as a temperature sensor in the stator frame. A resolver is a type of sensor commonly used in motor control systems to determine the precise angular position of the rotor. This information is essential for accurate control and operation of the motor [17].

The computational analysis was conducted without using the temperature sensor and thus considering there are no variations in temperature as well as phase inductances and resistance phase values. This indicates that in order to be even closer to the actual implementation, further development of the simulation is necessary to account for these addressed issues. The control scheme was designed to operate at a frequency of 16 kHz, and all the necessary calculations were performed using this data.

The motor's characteristics were extracted from the EMRAX 228 technical data sheet that can be seen in Appendix A. The datasheet presents a table including important information about the construction of the motor that was resumed in Table 4.1. This table shows the confirmation that the motor is a salient-free Permanent Magnet Synchronous Motor because of its near equal inductances in the direct and quadrature axes ($L_d = L_q$).

4.2   Simulation

To simplify the simulation environment, the system has been divided into subsystems that can be seen in Figure 3.2. Some of the subsystems or blocks are user-defined, meaning that the user defined all of the connections and equations, others are components that already exist in the Simulink library, allowing to keep the focus on the control system and use the Simulink Block Library to simplify the simulation. One example is the PMSM motor, where the block already implements the motor equations and the user only has to input the motor parameters in order to bring the simulation closer to the actual implementation.

Using Matlab code in conjunction with Simulink can greatly enhance the flexibility and customization of simulations, allowing the creation of code where parameters can be inputted and later used as predefined variables in the blocks present within the Simulink Library or in the overall simulation environment. By defining parameters and settings beforehand in Matlab Code, they can be easily modified if needed without directly modifying the Simulink model. This proves to be particularly useful when working with complex systems involving various components.

Table 4.1: EMRAX 228 High Voltage Technical Table - Important parameters used in the simulation

EMRAX 228 High Voltage Electrical Parameters	
Maximal battery voltage [Vdc] and max load [rpm]	680 Vdc (5500 RPM)
Peak motor power at max load RPM (few min at cold start / Few seconds at hot start) [kW]	109
Continuous motor power (at 5500 RPM) [kW]	62
Maximal rotation speed [rpm]	5500
Maximal motor current (for 2 min if cooled as described in Manual) [Arms]	240
Continuous motor current [Arms]	115
Maximal motor torque (for a few seconds) [Nm]	230
Continuous motor torque [Nm]	120
Internal phase resistance at 25ºC [mΩ]	16.7
Induction in L_d/L_q [μH] of 1 phase	177/183
Controller / motor signal	sine wave
Magnetic flux - axial [Vs]	0.0542
Number of pole pairs	10
Rotor inertia LC motor [kg*m^2]	0.0383

The used blocks from the library are listed below with the respective parameters, along with the code with the variables from the motor's technical sheet.

In the case of this specific application, some of the chosen components, such as the power converter and motor, were not developed from scratch but were selected to suit the application requirements. The approach involved designing the system using Simulink module blocks. This simplifies the simulation process by utilizing pre-built components that are readily available in the Simulink Library.

The MATLAB code [18], as shown in Figure 4.1, demonstrates the flexibility provided by defining motor parameters and control settings within the code such as the sampling time. These parameters, obtained from the motor's technical sheet, can be easily modified or replaced without directly modifying the Simulink model. The same happens for the controller gains.

```
1      clc;
2      clear;
3      close all;
4
5      %% PMSM Parameters
6      Ld = 177e-6; %H
7      Lq = 183e-6; %H
8      pole_pairs = 10; %pole pairs
9      Rs = 16.7e-3; %ohm
10     flux_link = 0.0542; %Wb
11
12
13     %% SETTINGS
14     Vdc = 600; %V
15
16     Load_Torque = 50; %Nm
17     N_ref = 1000; %rpm
18     wm_ref = N_ref * (pi/30); %rad/s
19
20     Ts = 2e-6; %s
21     TsC = 5*Ts; %s
22
23     Vph_max = Vdc * (1/sqrt(3));
24
25     %%Controller Gains
26     Kp_speed = 99.0375;
27     Ki_speed = 6.8873;
28
29     Kp_current = 84.45;
30     Ki_current = 13.3101;
31
```

Figure 4.1: Matlab code

4.2.1   Powergui

The powergui block is necessary for any simulation of a Simulink model that contains Simscape Electrical Specialized System blocks. It provides not only the solver options but also opens tools for steady-state and simulation results analysis. For optimal performance, it is recommended to place the powergui block in the top-level diagram of your Simulink model.

In this case, the discrete setting was used, indicating that the electrical system was discretized for a solution at fixed time steps which is particularly useful when implementing digital control algorithms.
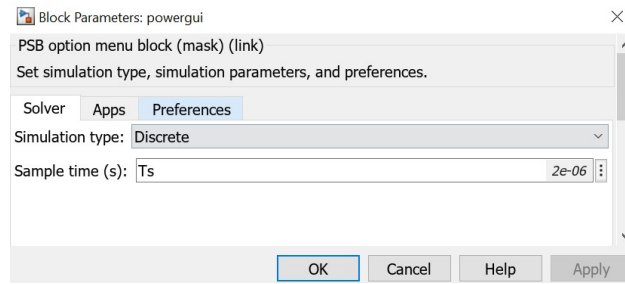

Figure 4.2: powergui block

Figure 4.3: powergui block parameters

As seen in Figure 4.3, the sample time parameter of the simulation is Ts, which was on the parameters defined in the Matlab code.

4.2.2   Permanent Magnet Synchronous Machine

The EMRAX228 was modeled through an existing block named Permanent Magnet Synchronous Machine, where the mathematical model of a three-phase or five-phase PMSM with sinusoidal is implemented with the stator windings connected in a star fashion to an internal neutral point just like the motor.

A three-phase sinusoidal model was selected within this block, thus implementing the following motor equations ([19]):

$$\frac{d}{dt}i_d = \frac{1}{L_d}v_d - \frac{R}{L_d}i_d + \frac{L_q}{L_d}p\omega_m i_q \tag{4.1}$$

$$\frac{d}{dt}i_q = \frac{1}{L_q}v_q - \frac{R}{L_q}i_q + \frac{L_d}{L_q}p\omega_m i_d - \frac{\lambda p\omega_m}{Lq} \tag{4.2}$$

$$T_e = 1.5p\left[\lambda i_q + (L_d - L_q)i_d i_q\right] \tag{4.3}$$

Where:

- L_d,L_q - d-axis and q-axis inductances

- R - Resistance of the stator windings

- i_d,i_q - d-axis and q-axis currents

- v_d,v_q - d-axis and q-axis voltages

- ω_m - Angular velocity of the rotor

- λ - Amplitude of the flux induced by the permanent magnets of the rotor in the stator phases

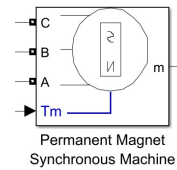- p - Number of pole pairs

- T_e - Electromagnetic torque

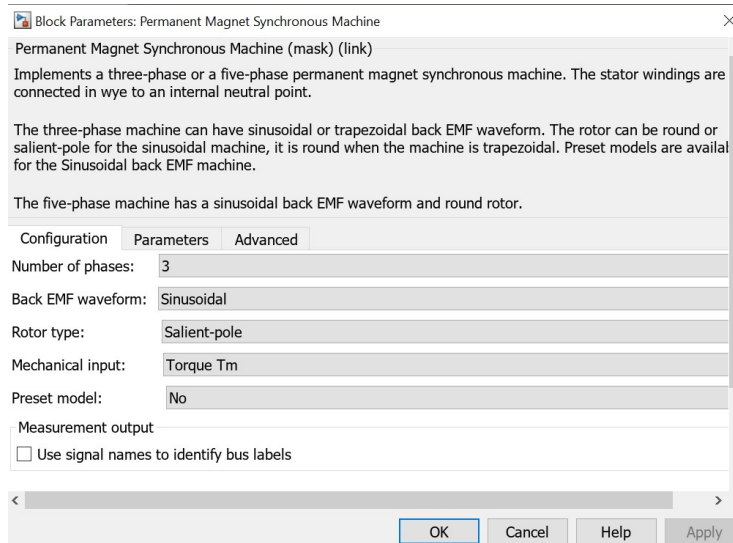Figure 4.4: Permanent Magnet Synchronous Machine block

Figure 4.5: Permanent Magnet Synchronous Machine block Configuration
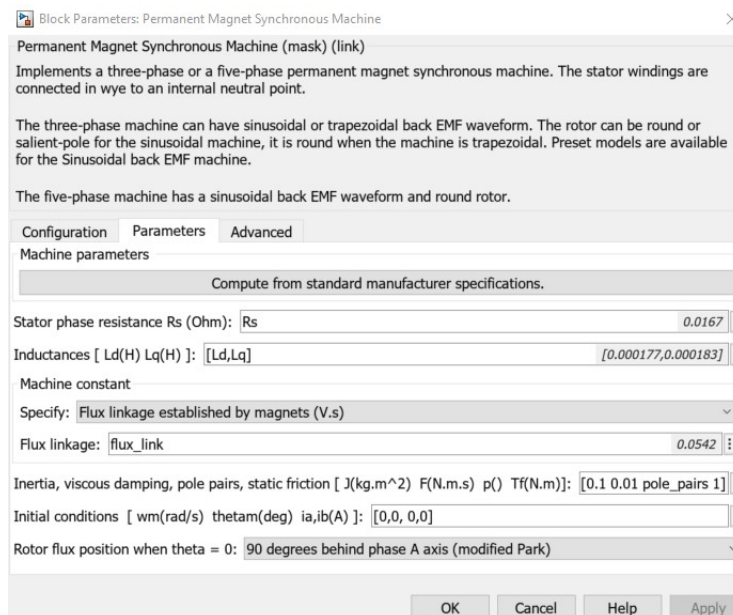

Figure 4.6: Permanent Magnet Synchronous Machine block Parameters

In Figure 4.5, the motor configuration was defined, and in Figure 4.6 the parameters were chosen. Most of them were defined in the Matlab code previously provided which were in turn obtained from the motor technical sheet.

4.2.3 Two-Level Converter

A two-level power converter is implemented where the switching devices model was selected. This means that IGBT/diode pairs are modeled and controlled by firing pulses from a PWM generator, providing the most accurate results. The firing pulses serve as an input in "g" (Figure 4.7). Another input is the DC link voltage and the output of the block are the three ports A,B, and C that will connect to the three phases of the motor ([20]).
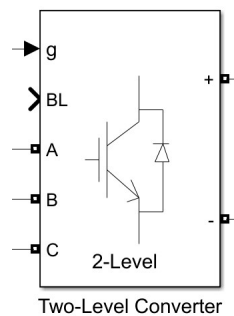

Figure 4.7: Two-level converter block
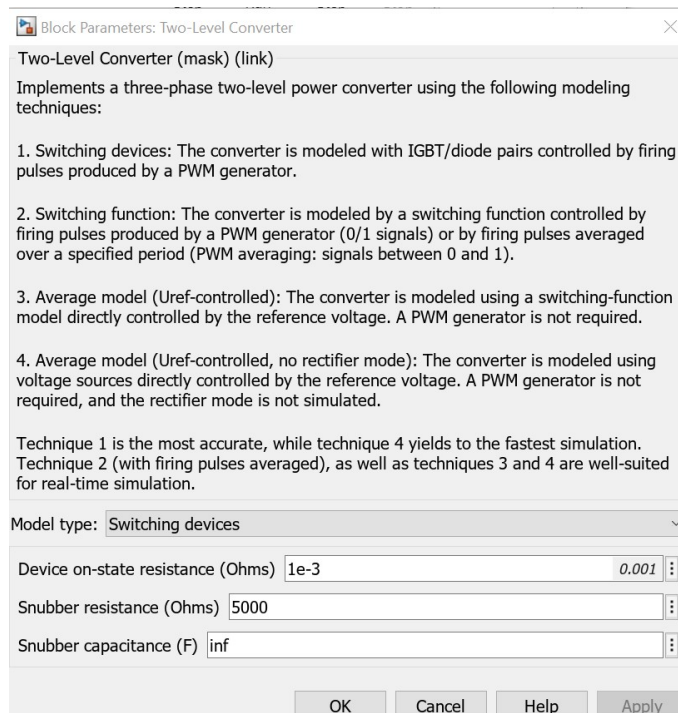
Figure 4.8: Two-level converter parameters

4.2.4   PWM Generator

The PWM Generator block creates the switching signals that serve as an input for the two-level converter. By calculating the on and off gating signals based on a DC-link voltage and on the three sinusoidal reference voltages. Then it uses the calculated gating signals to produce six switch-controlling pulses and finally generates modulation waveforms ([21]).

The block allows to define the PWM, and the sampling mode, incorporating SVM. The switching frequency is set to 16 kHz with a sampling time of T_s predefined in the Matlab code.

Figure 4.9: PWM Generator block

Figure 4.10: PWM Generator parameters

4.2.5 Reference Frame Transformations

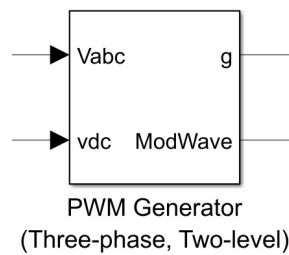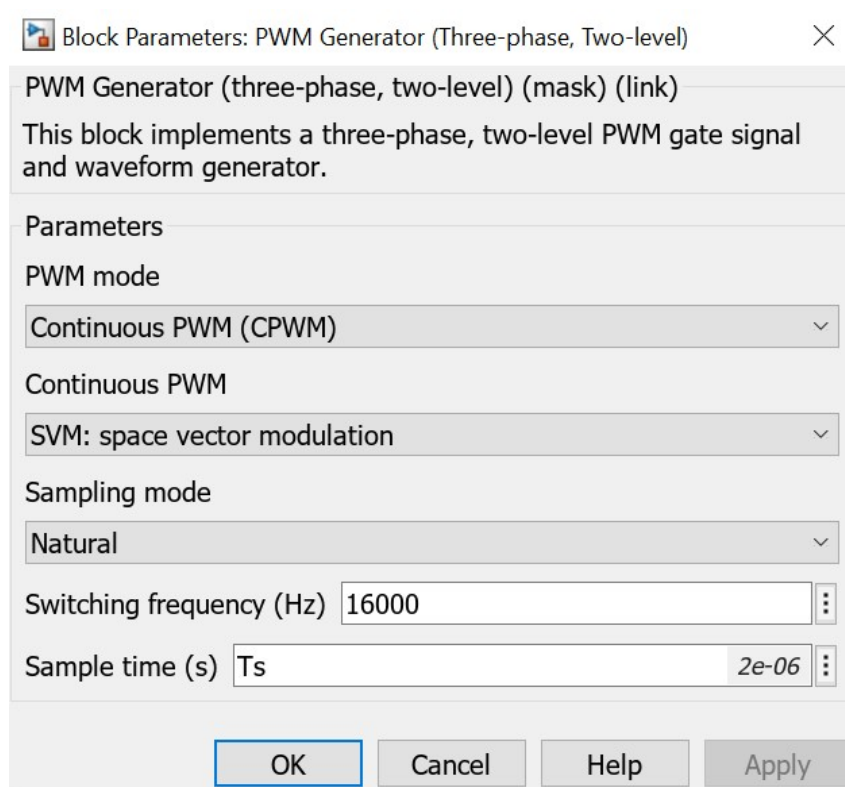To perform the reference frame transformations, a Simulink Library block is applied. This block, named Park Transform and Inverse Park Transform, first applies the Clarke transform in order to convert the three-phase quantities into two-phase represented in the $\alpha\beta$ reference frame. Then the park transform is applied to convert them into a rotating reference frame, as Chapter 2.4 explains.
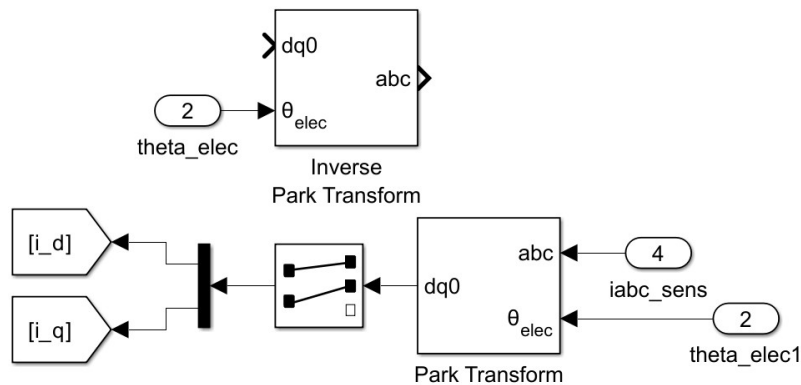
Figure 4.11: Reference Frame Transformations

Figure 4.11 shows the Inverse Park Transform that receives as an input the direct and quadrature axes reference values obtained by the control system and the measured electrical rotor angle and outputs the transformed abc values for the PWM generation. It can also be seen the Park Transform block where the direct and quadrature currents are obtained by the measured abc currents and electrical rotor angle inputs.

4.2.6 Angle and Speed Electrical Conversion

These conversion blocks implement simple functions to convert the mechanical angle and speed to the corresponding electrical values, needed to run calculations in the control system ([18],[22]).
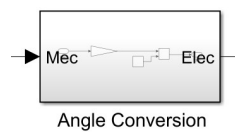
Figure 4.12: Angle Conversion Block

Figure 4.13: Angle Conversion Implementation
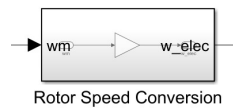
Figure 4.14: Rotor Speed Conversion Block
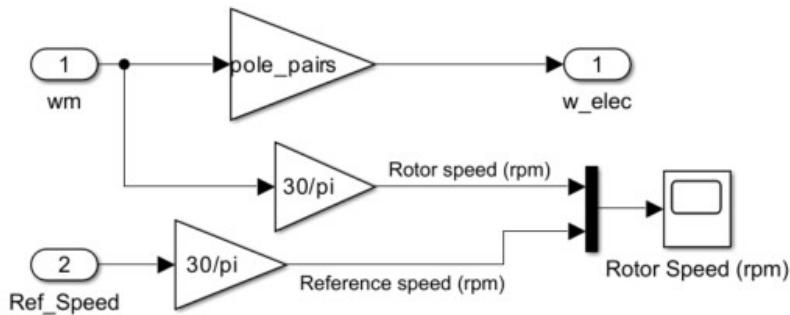
Figure 4.15: Rotor Speed Conversion Implementation

4.2.7 Speed Control Loop

The Speed Control Loop incorporates various components to achieve accurate speed regulation. First, a speed reference is generated based on driver commands. The actual motor speed is measured using a speed sensor, providing feedback information to obtain the speed error, calculated by comparing the desired reference and measured speed. In Figure 4.16, the speed control loop can be seen with the needed inputs such as the reference speed and the measured electric rotor speed. The output is the reference quadrature current for the following current control loop .
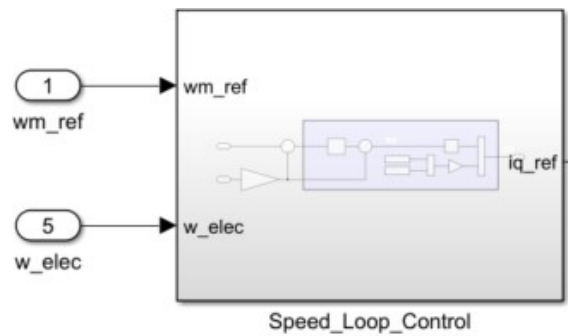
Figure 4.16: Speed Control Loop Block
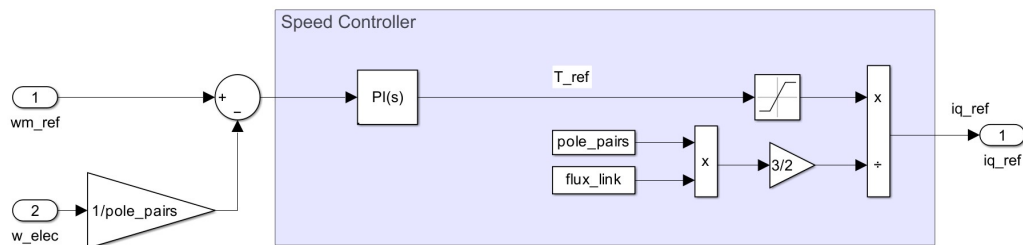
Figure 4.17: Speed Control Loop Implementation

Figure 4.17 shows the block implementation. First, the measured electrical angle is converted back to a mechanical angle so that can be compared to the reference speed input. The error is then fed to a PI controller which generates a control signal to adjust current commands.

4.2.8 Current Control Loop

The Current Control Loop in a motor drive system is a very important component responsible for regulating the motor's current according to desired objectives. This control loop utilizes feedback information from measured currents to compare them with the desired reference. By calculating the current error and employing a PI control strategy, it generates a control signal that adjusts the motor drive's output.

The block in Figure 4.18 has the direct and quadrature axes voltage values that are used in the Inverse Park Transform block and later in the PWM Generator block and receives five different inputs. These inputs are the direct and quadrature reference currents, as well as the direct and quadrature measured currents and the rotor electrical angle.
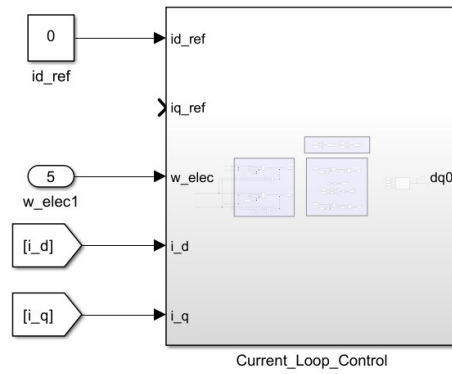
Figure 4.18: Current Control Loop Block
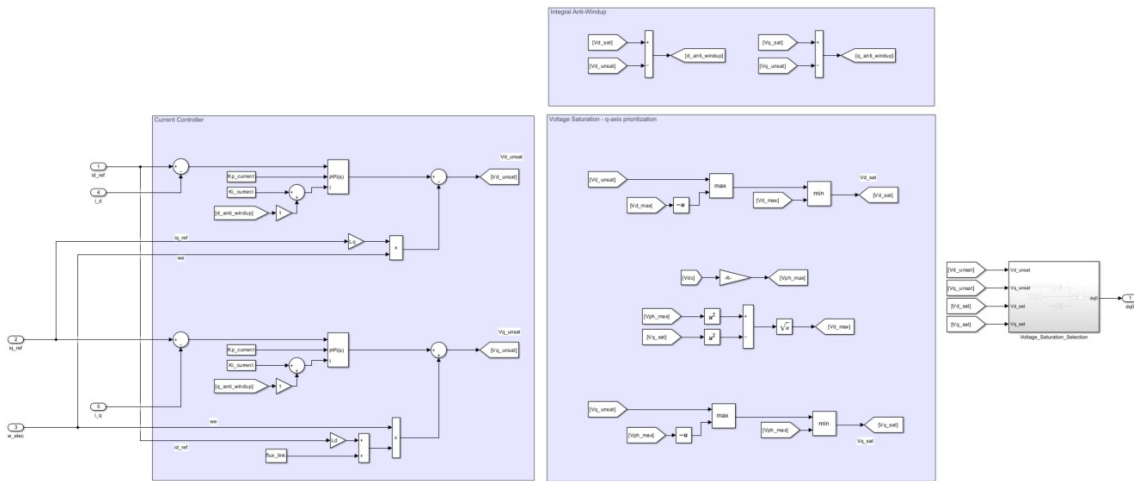
Figure 4.19: Current Control Loop - Layout

The block implementation is structured by a few sections. The first one is the Current Controller itself which is composed of two separate calculations for the direct and quadrature axes. The difference between the reference and measured currents is calculated and the error is fed to a PI controller on both axes. Then two different equations are implemented. They are, for the direct and quadrature axes respectively:

$$V_{d\_unsat} = \left(K_{p\_id} + K_{i\_id} \frac{1}{s} \right) i_{d\_error} - \left(i_{q\_ref} * L_q * w_e \right) \tag{4.4}$$

$$V_{q\_unsat} = \left(K_{p\_iq} + K_{i\_iq} \frac{1}{s} \right) i_{q\_error} + \left(w_e * \left(i_{d\_ref} * L_d + flux_{link} \right) \right) \tag{4.5}$$
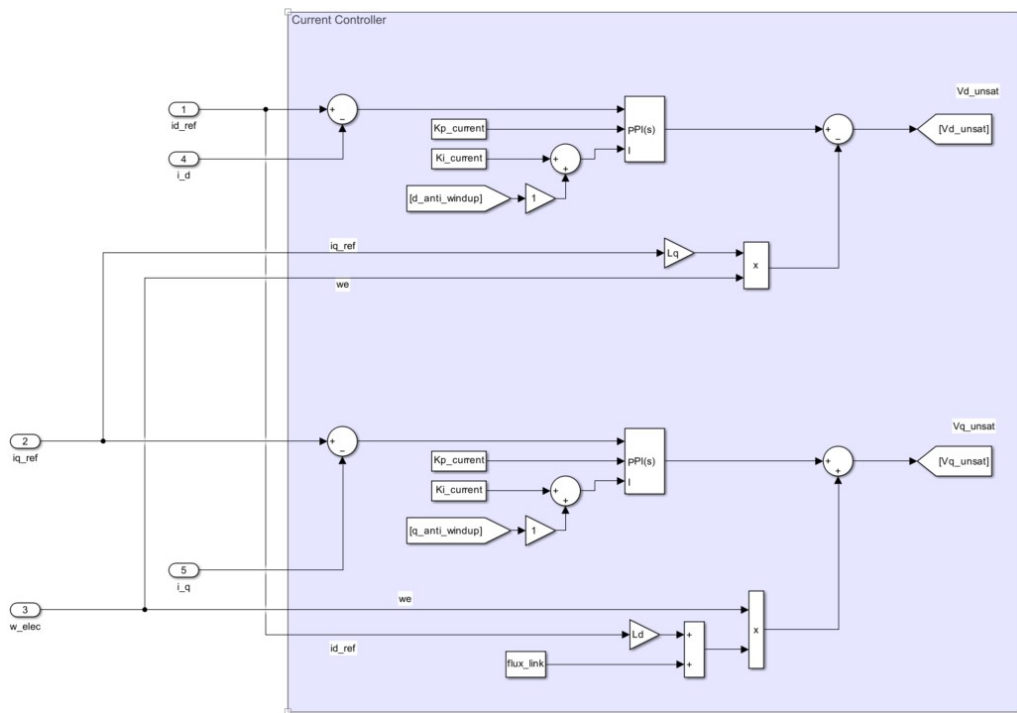
Figure 4.20: Current Control Loop - Current Controller Section

The current controller provides unsaturated voltages in both axes that need to be limited if the stator voltage surpasses its maximum ([23]).

Following a q-axis prioritization, the applied equations to saturate the voltage are:

$$v_d^{sat} = min\left(max\left(v_d^{unsat}, -V_{d\_max}\right), V_{d\_max}\right) \tag{4.6}$$

$$v_q^{sat} = min\left(max\left(v_q^{unsat}, -V_{ph\_max}\right), V_{ph\_max}\right) \tag{4.7}$$

Where

- v_d^{unsat} and v_q^{unsat} are the unsaturated voltages

- v_{d_max} is the maximum value that does not exceed the voltage phase limit and is given by the following equation: $v_{d\_max} = \sqrt{\left(V_{ph\_max}\right)^2 - \left(v_q^{sat}\right)^2}$

- v_{ph_max} is the voltage phase limit obtained through the DC link voltage: $v_{ph\_max} = \frac{V_{DC}}{\sqrt{3}}$
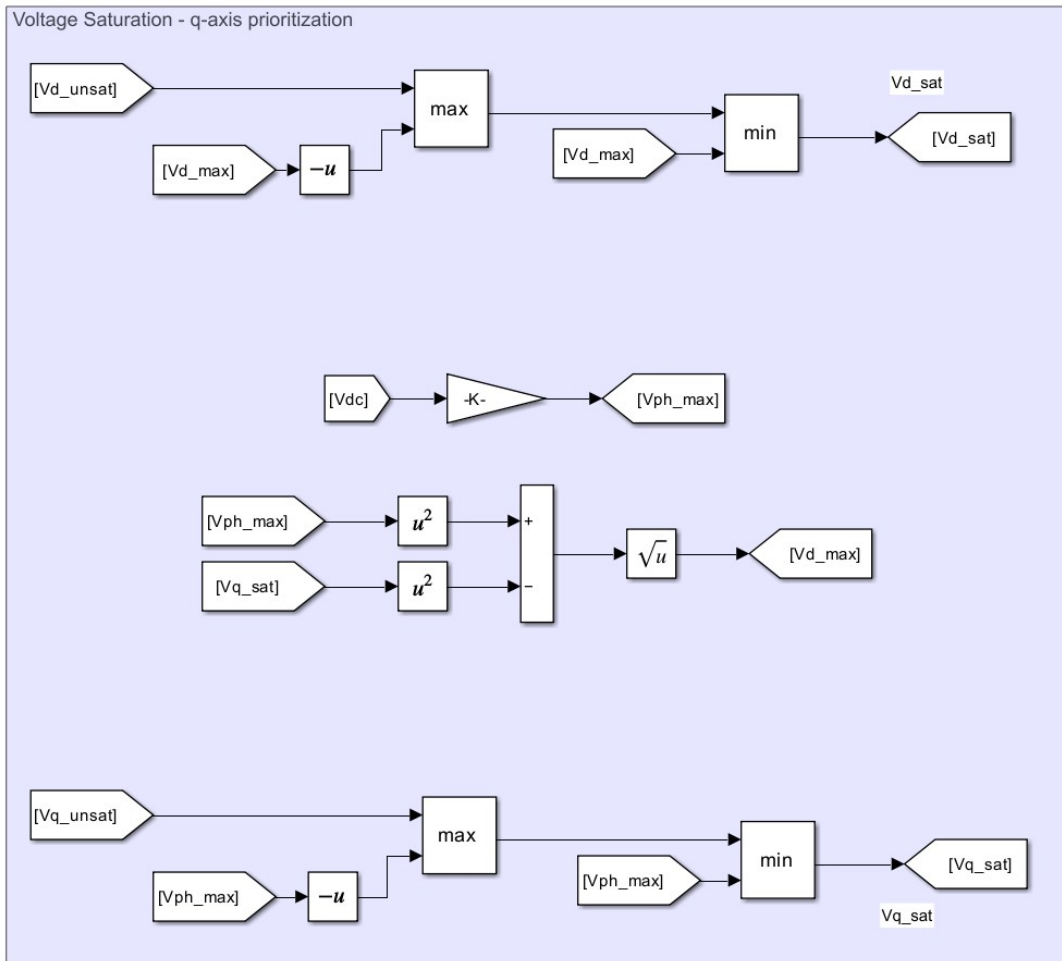
Figure 4.21: Current Control Loop - Voltage Saturation Section

Then a Voltage Saturation Selection block is implemented, which outputs saturated or unsaturated voltages from the previous sections through a simple condition (equation 4.8). Its implementation can be seen in Figure 4.23 ([23]).

$$\sqrt{v_d^2 + v_q^2} \leq V_{ph\_max} \tag{4.8}$$
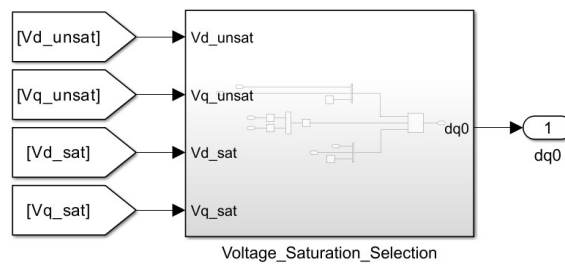
Figure 4.22: Current Control Loop - Voltage Saturation Selection block
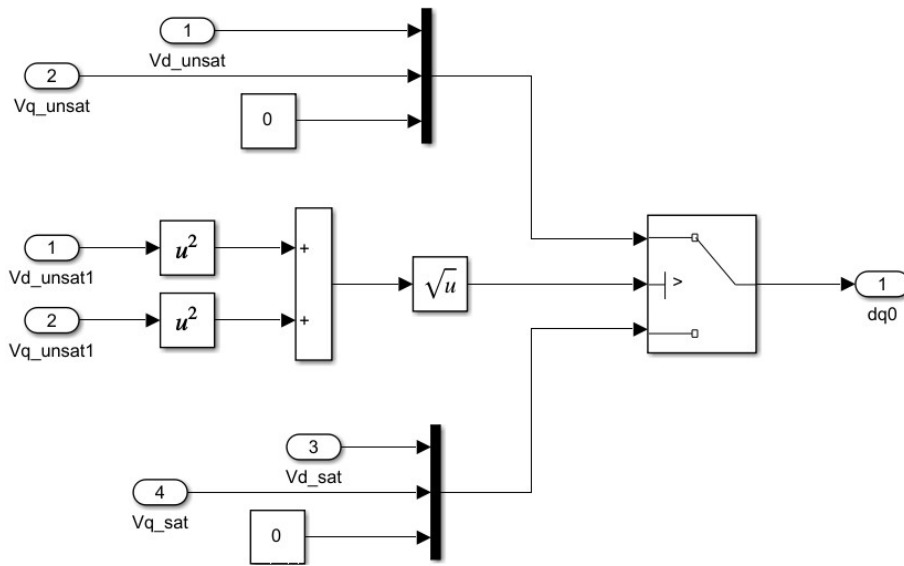
Figure 4.23: Current Control Loop - Voltage Saturation Selection Implementation

To finalize the Current Control Loop, an Integral Anti-Windup mechanism was set up. This prevents saturation in the integrator output which otherwise can lead the control system to poor performance, instability, or even system failure. When saturation occurs, the controller's integral component can continue to accumulate the error, causing it to overshoot or to have a slow response. Employing this mechanism limits the integration action when saturation occurs. Overall, it is advantageous because it provides a better control system behavior and by preventing the adverse effects of windup.

The execution is done by altering the controller integral gain. The controller proportional and integral gains now become ([23]):

$$K_{i\_id} + K_{aw\_id} \left(v_d^{sat} - v_d^{unsat} \right) \tag{4.9}$$

$$K_{i\_iq} + K_{aw\_iq} \left(v_q^{sat} - v_q^{unsat} \right) \tag{4.10}$$

Where

- K_{aw_id} and K_{aw_iq} are the anti-windup gains for each axis.

The difference between saturated and unsaturated values was calculated in Figure 4.24 and then *d_anti_windup* and *q_anti_windup* were added to the Integral gain of each axis PI controller as can be seen in Figure 4.20.
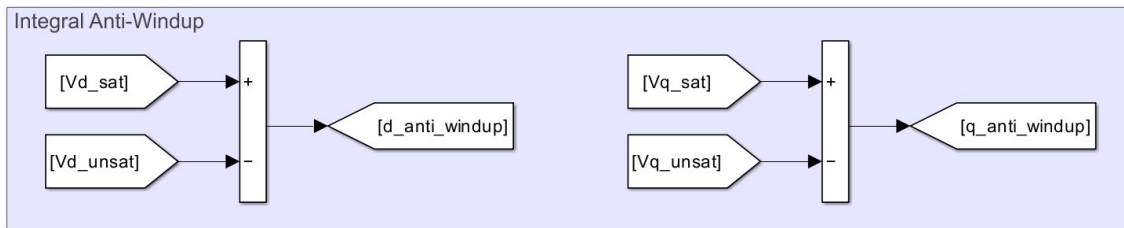
Figure 4.24: Current Control Loop -Integral Anti-Windup Implementation

4.3   Initial Results

A initial test was conducted with the controller gains values listed below in order to validate the system operation, verifying that everything was working as expected and also to obtain a base scenario that could be later optimized.

The base scenario simulation results presented in Figure 4.25 show the behavior of the system for a speed reference of 1000 rpm and a total simulation time of 0.1s. On top, it can be seen the rotor speed in rpm and its reference, followed by the electromagnetic torque obtained from the motor, and finally the measured stator currents.

The base scenario speed and current controller proportional and integral gains are:

- $Speed_{Kp} = 10$

- $Speed_{Ki} = 100$

- $Current_{Kp} = 10$

- $Current_{Ki} = 100$

Where Kp is for the proportional gain and Ki is for the integral gain.

It is clear that the control system presents very poor performance due to the very slow convergence and the overshoot of the speed reference, on the other hand, the measured stator currents provide promising results, revealing insightful information that the system is actually working as intended.

Figure 4.25: Base Scenario

After the initial test was conducted and the base scenario was created, the system response could be improved. This was done by maintaining both speed reference and total simulation time, and by altering the speed and current controller gains. The approach was to try various different values and after several iterations, the obtained gains that showed the best results were:

- $Speed_{Kp} = 20$

- $Speed_{Ki} = 10$

- $Current_{Kp} = 40$

- $Current_{Ki} = 1$

The results for the manual optimization conducted on the parameters can be seen in Figure 4.26 which shows a big improvement in the system's response. The motor reaches the reference speed much faster only slightly overshooting it and torque can be reduced earlier.

Figure 4.26: Manual Optimization Scenario

4.4   Controller Gains Optimization

The improvement obtained earlier just by manually changing values was very good. So, the opportunity to further optimize these values computationally only made sense.
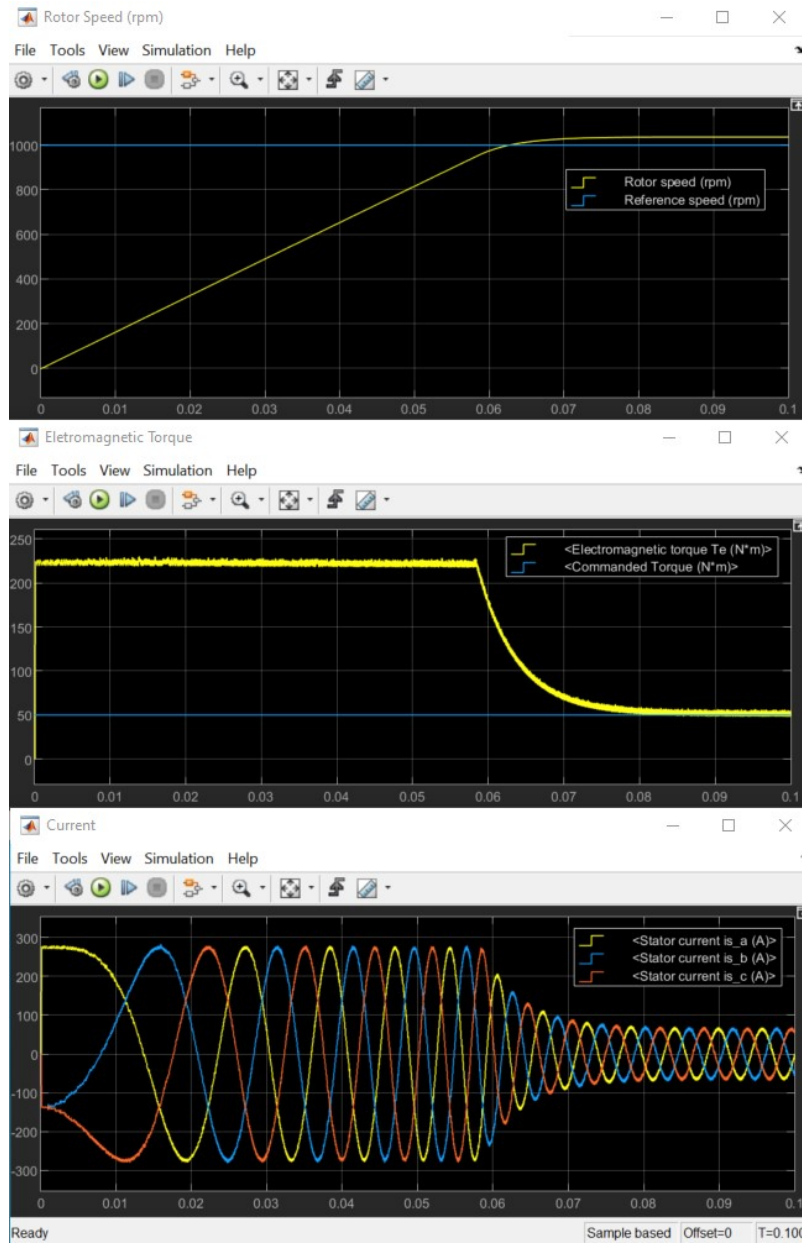
Taking advantage of the Matlab code interface, the goal was to write a small code that would implement the control system and provide values for a given optimization. Particle Swarm Optimization (PSO) was chosen. It is a popular and effective optimization method used in several applications, including control system parameter tuning. A few other optimization methods were considered and rudimentary tests were conducted on Genetic Algorithms (GA) and Gradient-Based Optimization, but the most promising results were obtained from the use of PSO.

PSO is an optimization algorithm that leans on mimicking birds, fishes, and insect's social behavior [24]. It is an evolutionary and stochastic algorithm where several candidate solutions are processed simultaneously by random. The collection of particles is randomly distributed and confined into a search space, where each particle evaluates its current position. Then, over a pre-defined number of iterations, they dynamically update their positions in search of better fitness. Each particle's movement is influenced by its own best-known position and the best-known position can be reached by any particle in the swarm. When considering historical positions, the particles adjust their velocity, moving towards potentially more promising regions. To prevent the swarm from converging to a suboptimal solution, random perturbations are introduced [25].

According to reference [24] a common population selection would be from twenty to fifty particles. In this case, the best results were obtained from a population of fifteen with twenty-five iterations.

The PSO algorithm follows these steps [25]:

- Initialization - Randomly initialize the particle's position and velocities in the search space

- Fitness Evaluation - Evaluate the objective function for each particle to determine its fitness

- Compare and Update - Based on each particle's current fitness, update the personal best position if it has better fitness than the previous best. Global Best must also be updated in the same condition

- Update Velocity and Position - Update the velocities and positions of the particles based on their current velocities, and positions. The new velocity is influenced by both the particle's previous velocity and the distances to its best positions.

- Repeat steps 2-4 - Iterate until the maximum number of iterations has been met

In summary, PSO harnesses collaboration and communication among particles to improve their positions and achieve the best fitness by each iteration. It balances exploration and exploitation by combining historical information with random perturbations, leading to an efficient search for the most optimal solution within the defined problem space.

As this optimization relies on randomization of the search space, it is normal for the algorithm to deliver different values each time the code was run. This meant that the code (Appendix B) had to be executed several times so it could produce a wide range of values. These values served later as parameters to be tested in the control algorithm. After all the extracted values from the code were tested, the speed and current controller gains that showed better performance were:

- $Speed_{Kp} = 99.0375$

- $Speed_{Ki} = 6.8873$

- $Current_{Kp} = 84.45$

- $Current_{Ki} = 13.3101$

The results obtained from these gains can be seen in Figure 4.27. It presents a much higher speed accuracy. The yellow line on the top image is very close to the speed reference. In the elec- tromagnetic torque middle image, a huge improvement is clear, without overshooting it responds very rapidly returning to the load torque, in blue, very quickly.
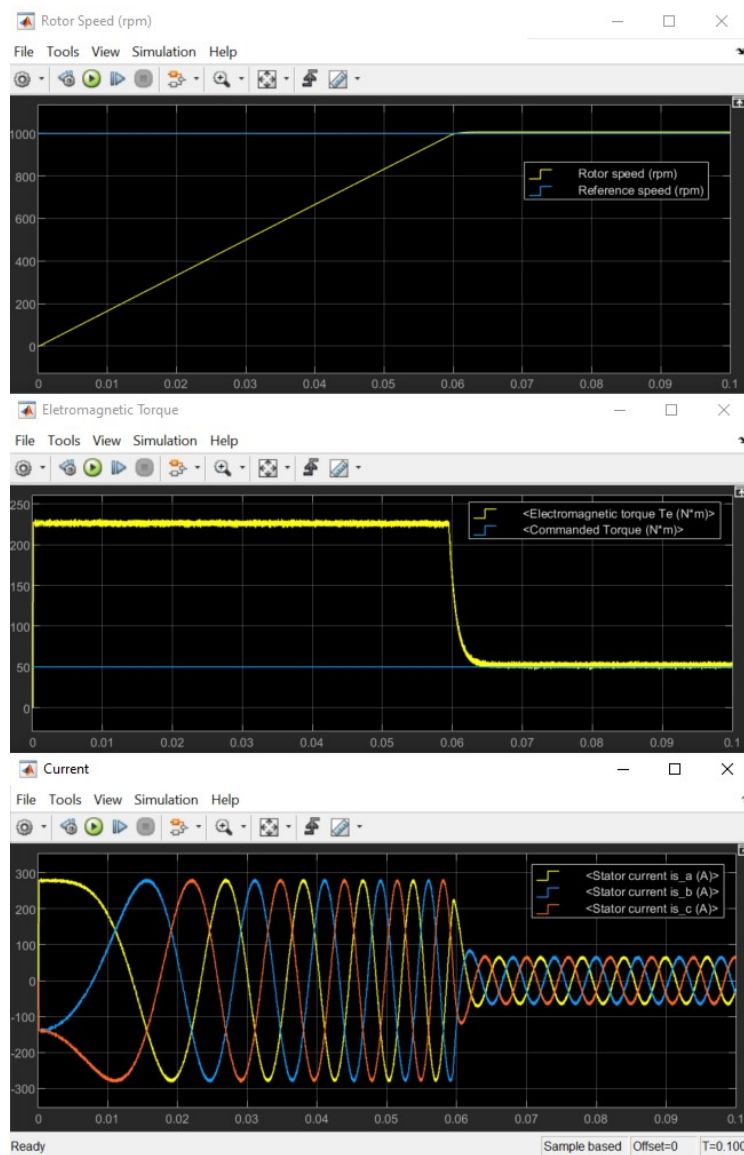
Figure 4.27: PSO Optimization Scenario

4.5   Simulation Final Remarks

For a Formula Student type car and the event that this dissertation focuses on, which is an acceleration test over a distance of seventy-five meters, the vehicle must accelerate full throttle and get there as fast as possible. As the acceleration test is conducted over a short period of time, it would make sense to discard the speed controller, and the motor could run at full power and speed for a few seconds to obtain the best results.

However, one could also run the motor at a reference speed that could approximate its peak power. Analyzing the data provided for the EMRAX 228, seen in Appendix A, a value for the speed near its peak power and torque is 5000 rpm. By running the motor in these conditions, the speed controller could be kept functioning inside the control system. In Figure 4.28 can be seen the motor delivering the maximum torque possible for this motor, until it reaches the speed reference of 5000 rpm.
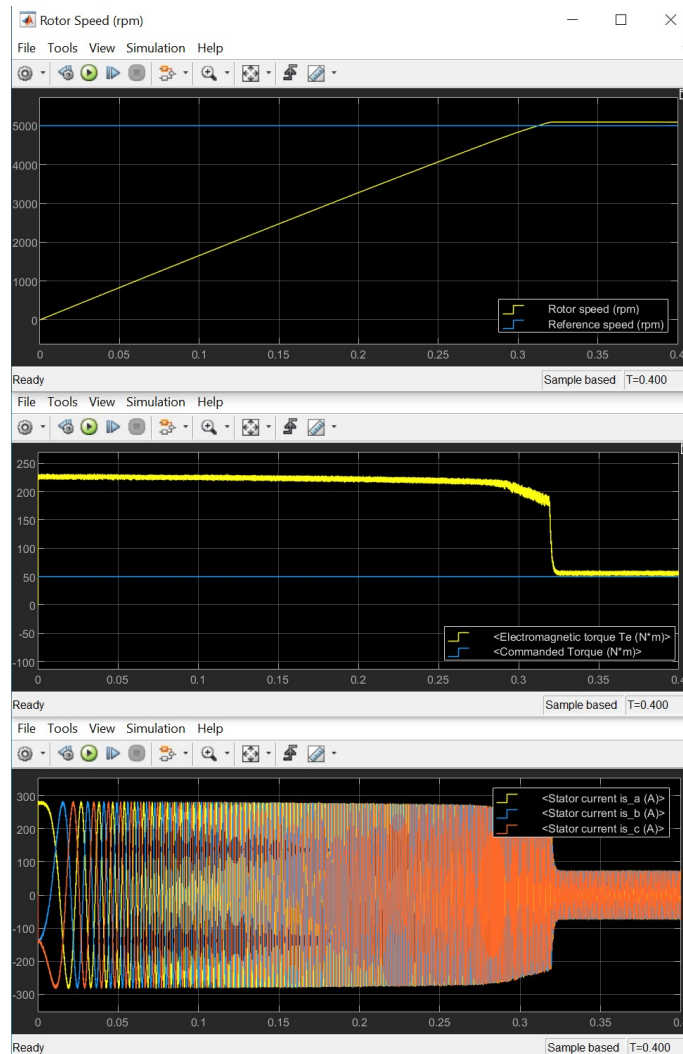
Figure 4.28: Simulation results 5000rpm

There are a few advantages to this approach listed below:

- Modular Design - The inclusion of a speed controller in the system enables a modular design approach that allows seamless integration and expansion with other control modules, facilitating the inclusion of new features or functionalities without major redesign. The modularity ensures high flexibility and adaptability for future implementations.

- Cruise Control Integration - A potential feature implementation is the integration of a cruise control feature. Having the speed controller already implemented allows for easier incorporation of cruise control functionality into the system. The speed controller can be extended to support this feature with the appropriate algorithms and interfaces, allowing the vehicle to maintain a constant speed without the driver continuously applying throttle, providing comfort and enhancing the overall driving experience.

- Speed Limiting and Regulation - Another example is the usage of a speed controller to limit the speed and regulate it. By adding appropriate algorithms and user interfaces, the system can be expanded to include features like speed limiters, where the maximum vehicle speed can be set and adjusted as per safety requirements or regulations, ensuring compliance with speed limits and overall vehicle safety.

- Advanced Driver Assistance Systems (ADAS) - The control system can be a foundational component for advanced driver assistance systems. The possibility to integrate it with sensor-based technologies, such as radar or cameras, the controller can be a part of a broader ADAS framework. It can contribute, for example, to functionalities like adaptive cruise control, where the vehicle automatically adjusts its speed based on the distance of the vehicle ahead, boosting safety.

- Autonomous Vehicle Integration - As autonomous vehicles evolve, the ability to precisely control the vehicle's speed without driver input becomes even more critical and the inclusion of the speed controller lays the groundwork for potential integration with autonomous vehicle technologies. By leveraging the existing speed controller, the traction control system can become a key component in autonomous driving systems, facilitating the accurate control of vehicle speed in various driving scenarios.

It is clear the speed controller should be considered as it provides scalability for the system and enhances the possibilities of the project providing not only the safety aspect but the performance and adaptability. With its modularity, one can also see the potential for future implementations and advancements with other systems, making it feasible for commercialization.

Chapter 5

Conclusion and Future Considerations

5.1 Conclusion

This Dissertation focused on the development and implementation of a traction control system for a Formula Student type car. The Formula Student competition served as a foundation to understand the importance of advanced control systems in high-performance vehicles as well as the advantages obtained when using a traction control system.

The selection of a Permanent Magnet Synchronous Motor proved to be a suitable choice due to its high efficiency, controllability, and torque density, allowing high power outputs for an overall small and light motor.

A substantial amount of research was conducted on varied control algorithms and strategies, ultimately leading to Field Oriented Control with a speed control loop and a cascaded current control loop. The control strategy adopted was the Constant Torque-Angle Control which showcased very good performance in terms of torque control coupled with a simpler modulation design, advantageous as budget and simplicity were considered.

A comprehensive simulation model was created in Simulink, consolidating the entire control system and validating the effectiveness of the selected control strategy. The initial simulation results showed promising results. Using an optimization algorithm, the controller gains were improved, resulting in an outstanding system response.

This research not only adds value to the field of motorsport engineering but also introduces potential applications in road vehicle safety and performance enhancement as electric vehicles emerge in the market. The developed traction control system has the potential to improve the stability, and overall safety of commercial vehicles, thereby reducing accidents and boosting driver confidence.

In conclusion, this thesis has successfully achieved its objective of developing a traction control system for a Formula Student type car with a focus on the control system with very good performance. The research has contributed to the advancement of control strategies in high-performance vehicles and has the potential to make a positive impact on road vehicle safety and performance.

5.2   Future Considerations

As electric platforms are gaining a high amount of interest and more manufacturers from several different sectors are seeking the development of electric motors, control theories, efficiency in existing platforms, and battery technology advancements, it is important to pursue new ways to scale these systems with an aim in electrification.

Unfortunately, due to the scope of this project and time constraints, not all ideas were possible to complete, and thus some objectives to enhance this project are listed below:

- Improve the control system by combining it with other variables to take into account non-linear behavior such as resistance variation with temperature and magnetic saturation.

- Implement the control system in a development environment to try and run the motor with a microcontroller unit

- Once the control system is up and running with the microcontroller, develop a specific PCB with all the needed connections and components to later place it in the actual Formula Student car and obtain a performance validation.

- Add features to the control system allowing it to handle regenerative braking and simulating a battery pack so that the behavior towards its discharge provides a real-world scenario.

- Study the possibility to combine this project with other systems such as Advanced Driver Assistance Systems framework, for adaptive cruise control, autonomous driving, and others.

Appendix A

EMRAX 228 Technical Characteristics

EMRAX 228 Technical Data Table (dynamometer test data)

Technical data	EMRAX 228 High Voltage			EMRAX 228 Medium Voltage			EMRAX 228 Low Voltage		
Air cooled = AC / Liquid cooled = LC / Combined cooled = Air + Liquid cooled = CC	AC	LC	CC	AC	LC	CC	AC	LC	CC
Ingress protection	IP21	IP65	IP21	IP21	IP65	IP21	IP21	IP65	IP21
Cooling medium specification (Air Flow = AF; Inlet Water/glycol Flow = WF; Ambient Air = AA) If inlet WF temperature and/or AA temperature are lower, then continuous power is higher.	AF=20m/s AA=25°C	WF=8l/min at 50°C; AA=25°C	WF=8l/min at 50°C; AA=25°C	AF=20m/s AA=25°C	WF=8l/min at 50°C; AA=25°C	WF=8l/min at 50°C; AA=25°C	AF=20m/s AA=25°C	WF=8l/min at 50°C; AA=25°C	WF=8l/min at 50°C; AA=25°C
Weight [kg]	12,0	12,4	12,3	12,0	12,4	12,3	12,0	12,4	12,3
Diameter ø / width [mm]	228 / 86								
Maximal battery voltage [Vdc] and max load RPM	680 Vdc (5500 RPM)			500 Vdc (5500 RPM)			160 Vdc (5500 RPM)		
Peak motor power at max load RPM (few min at cold start / few seconds at hot start) [kW]	109								
Continuous motor power (at 5500 RPM)	50	53	62	50	53	62	50	53	62
Maximal rotation speed [RPM]	5500 (6500 for a few seconds with magnetic field weakening)								
Maximal motor current (for 2 min if cooled as described in Manual) [Arms]	240			340			900		
Continuous motor current [Arms]	115			160			450		
Maximal motor torque (for a few seconds) [Nm]	230								
Continuous motor torque [Nm]	96	102	120	96	102	120	96	102	120
Torque / motor current [Nm/1Aph rms]	1,1			0,75			0,27		
Maximal temperature of the copper windings in the stator and max. temperature of the magnets [°C]	120								
Motor efficiency [%]	92-98%								
Internal phase resistance at 25 °C [mΩ]	16,7			7,0			1,1		
Input phase wire cross-section [mm²]	11,4			17,0			42,5		
Wire connection	star								
Induction in Ld/Lq [µH] of 1 phase	177/183			76/79			10,3/10,6		
Controller / motor signal	sine wave								
AC voltage between two phases [Vrms/1RPM]	0,0730			0,0478			0,0176		
Specific idle speed (no load) [RPM/1Vdc]	9,8			14			40		
Specific load speed (max load) [RPM/1Vdc]	8			11			34		
Magnetic field weakening (for higher RPM at the same power and lower torque) [%]	up to 100								
Magnetic flux – axial [Vs]	0,0542			0,0355			0,0131		
Temperature sensor on the stator windings	kty 81/210								
Number of pole pairs	10								
Rotor inertia LC motor [kg*m²]	0,0383								
Bearings (front:back) - FAG	6206:3206 (for axial-radial forces; for pull-push mode, α=25°)								

Figure A.1: EMRAX 228 Technical Data Table
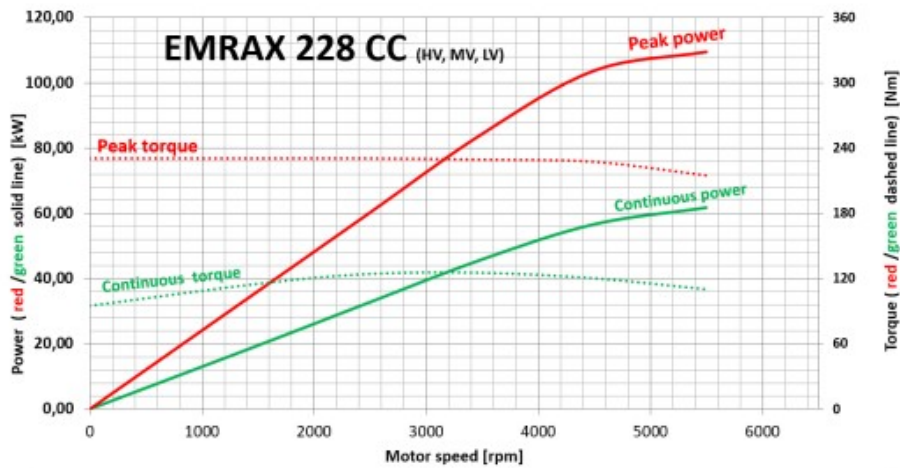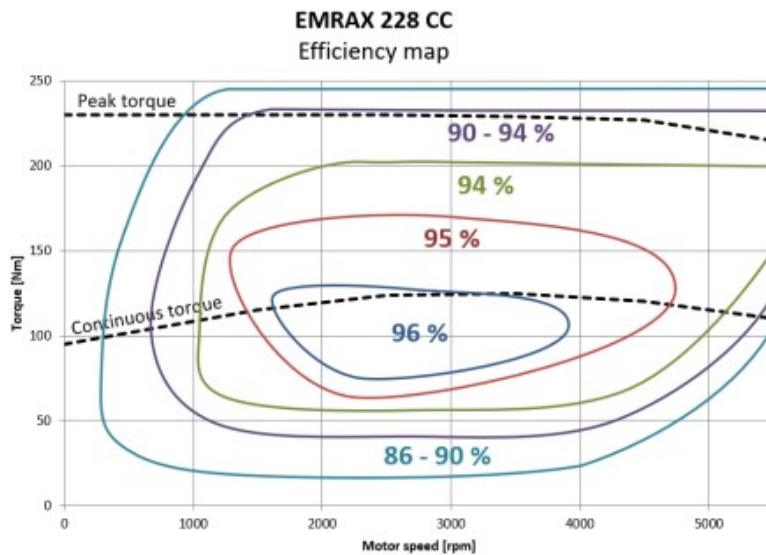
Figure A.2: EMRAX 228 Power/Torque Graph and Efficiency Map
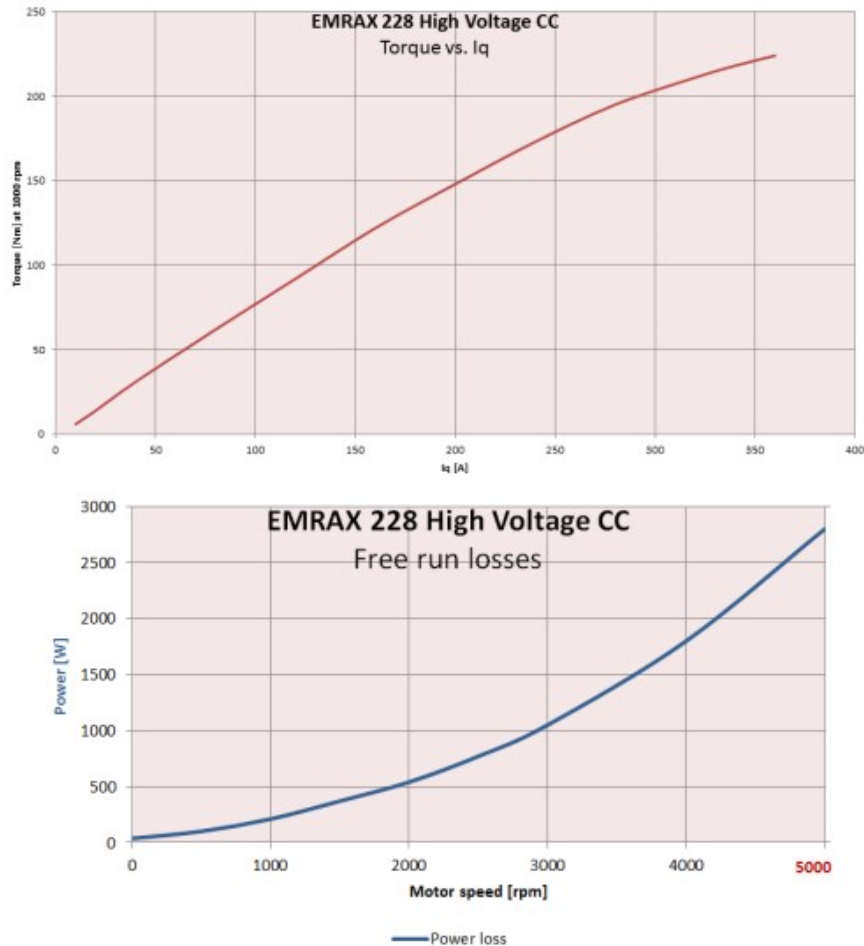
Graphs of EMRAX air cooled and liquid cooled type:
The continuous power and continuous torque for air cooled motor is 20% lower and for liquid cooled motor is 15% lower.

Graphs of the EMRAX 228 medium and low voltage motor type:
Graphs of EMRAX 228 low voltage and EMRAX 228 medium voltage are similar to graphs of EMRAX 228 high voltage. The only differences are the DC voltage and motor current. These two parameters can be read from the Technical data table for the EMRAX 228 low and medium voltage motor.
Low voltage motor needs 4 x higher current and 4 x lower DC voltage for the same power/torque and RPM, compared to EMRAX 228 high voltage motor.
Medium voltage motor needs 1.52 x higher motor current and 1/3 lower DC voltage for the same power/torque and RPM, compared to EMRAX 228 high voltage motor.

www.emrax.com   **20**

Figure A.3: EMRAX 228 Toque/Current Graph

Appendix B

Controller Gains Optimization MATLAB code

```
1    clc;
2    clear;
3    close all;
4
5    % Motor Parameters
6    R = 16.7e-3;              % Phase Resistance (ohm)
7    Ld = 177e-6;             % Direct-axis Inductance (H)
8    Lq = 183e-6;             % Quadrature-axis Inductance (H)
9    J = 0.0383;              % Rotor Inertia (kg*m^2)
10
11   % PSO Parameters
12   numParticles = 15;       % Number of particles in the swarm
13   maxIterations = 25;      % Maximum number of iterations
14   c1 = 1.5;                % Cognitive parameter
15   c2 = 1.5;                % Social parameter
16   w = 0.7;                 % Inertia weight
17
18   % Define the objective function
19   objectiveFunction = @(x) simulateFOC(x(1), x(2), x(3), x(4), Lq, Ld, R, J);
20
21   % Define the bounds for the gains [Kp_speed Ki_speed Kp_current Ki_current]
22   lowerBounds = [1e-20 1e-20 1e-20 1e-20];
23   upperBounds = [100 100 100 100];
24
25   % Run PSO optimization
26   options = optimoptions('particleswarm', 'SwarmSize', numParticles, 'MaxIterations', maxIterations);
27   [bestGains, ~] = particleswarm(objectiveFunction, length(lowerBounds), lowerBounds, upperBounds, options);
28
29   % Display the best gains
30   disp('Optimized Gains:');
31   disp(['Kp_speed: ', num2str(bestGains(1))]);
32   disp(['Ki_speed: ', num2str(bestGains(2))]);
33   disp(['Kp_current: ', num2str(bestGains(3))]);
34   disp(['Ki_current: ', num2str(bestGains(4))]);
35
36   % Call the simulateFOC function with the best gains
37   performance = simulateFOC(bestGains(1), bestGains(2), bestGains(3), bestGains(4), Lq, Ld, R, J);
38
39   % Display the performance metric
40   disp('Performance Metric:');
41   disp(['Tracking Error: ', num2str(performance)]);
```

Figure B.1: Optimization Code - Part 1

```matlab
42
43     % Function to simulate FOC with given gains and return the performance metric
44     function performance = simulateFOC(Kp_speed, Ki_speed, Kp_current, Ki_current, Lq, Ld, R, J)
45         % Simulation Parameters
46         Ts = 2e-6;                    % Sampling time (s)
47         tFinal = 0.4;                  % Simulation time (s)
48         motorSpeedRef = 5000;        % Desired motor speed (rpm)
49
50         % Calculate speed reference in rad/s
51         motorSpeedRef = motorSpeedRef * (2*pi/60);
52
53         % Initialize variables and parameters
54         i_d = 0;
55         i_q = 0;
56         omega_e = 0;
57         omega_m = 0;
58         error_speed = 0;
59         integral_speed = 0;
60         error_current_d = 0;
61         integral_current_d = 0;
62         error_current_q = 0;
63         integral_current_q = 0;
64
65         % Simulation loop
66         for k = 1:(tFinal/Ts)
67             % Speed control
68             error_speed = motorSpeedRef - omega_m;
69             integral_speed = integral_speed + error_speed * Ts;
70             u_speed = Kp_speed * error_speed + Ki_speed * integral_speed;
71
72             % Current control
73             i_q_ref = u_speed;  % Use speed control output as reference for i_q
74
75             error_current_d = 0 - i_d;
76             integral_current_d = integral_current_d + error_current_d * Ts;
77             u_current_d = Kp_current * error_current_d + Ki_current * integral_current_d;
78
79             error_current_q = i_q_ref - i_q;
80             integral_current_q = integral_current_q + error_current_q * Ts;
81             u_current_q = Kp_current * error_current_q + Ki_current * integral_current_q;
82
83             % Calculate currents and update states
84             i_d = i_d + (u_current_d - Lq * omega_e * i_q - R * i_d) * Ts / Ld;
85             i_q = i_q + (u_current_q - Ld * omega_e * i_d - R * i_q) * Ts / Lq;
86
87             % Calculate electrical and mechanical speeds
88             omega_e = omega_e + (Ld * i_q * i_d - omega_e * (Lq * i_q^2 + Ld * i_d^2) - omega_m * J) * Ts / (J * Lq);
89             omega_m = omega_m + omega_e * Ts;
90         end
91
92         % Calculate performance metric (tracking error)
93         performance = abs(motorSpeedRef - omega_m * (60 / (2*pi)));
94     end
```

Figure B.2: Optimization Code - Part 2

References

[1] Felix Collin. Traction control for kth formula student, 2020.

[2] Hiroshi Fujimoto, Junya Amada, and Kenta Maeda. Review of traction and braking control for electric vehicle. In *2012 IEEE Vehicle Power and Propulsion Conference*, pages 1292–1299. IEEE, 2012.

[3] Formula student. URL: https://www.imeche.org/events/formula-student.

[4] Formula student - rules 2023. URL: https://www.imeche.org/events/formula-student/team-information/rules.

[5] Julio A Sanguesa, Vicente Torres-Sanz, Piedad Garrido, Francisco J Martinez, and Johann M Marquez-Barja. A review on electric vehicles: Technologies and challenges. *Smart Cities*, 4(1):372–404, 2021.

[6] Mehrdad Ehsani, Yimin Gao, Stefano Longo, and Kambiz M Ebrahimi. *Modern electric, hybrid electric, and fuel cell vehicles*. CRC press, 2018.

[7] Arun Eldho Aliasand and FT Josh. Selection of motor for an electric vehicle: A review. *Materials Today: Proceedings*, 24:1804–1815, 2020.

[8] Austin Hughes and Bill Drury. *Electric motors and drives: fundamentals, types and applications*. Newnes, 2019.

[9] URL: https://www.nde-ed.org/Physics/Magnetism/CoilField.xhtml.

[10] Gopal K Dubey. *Fundamentals of electrical drives*. CRC press, 2002.

[11] Bogdan M Wilamowski and J David Irwin. *Power electronics and motor drives*. CRC Press, 2018.

[12] Surajit Chattopadhyay, Madhuchhanda Mitra, Samarjit Sengupta, Surajit Chattopadhyay, Madhuchhanda Mitra, and Samarjit Sengupta. *Electric power quality*. Springer, 2011.

[13] MANISH TRIVEDI and RITESH KESHRI. Comparative evaluation of abc and stationary frame of reference for permanent magnet brushless dc motor drive applied for generation of switching pattern. *Turkish Journal of Electrical Engineering and Computer Sciences*, 27(6):4715–4730, 2019.

[14] Luis T Aguilar, Ramon Ramírez-Villalobos, A Ferreira de Loza, and Luis N Coria. Robust sensorless speed tracking controller for surface-mount permanent magnet synchronous motors subjected to uncertain load variations. *International Journal of Systems Science*, 51(1):35–48, 2020.

[15] Ramu Krishnan. *Permanent magnet synchronous and brushless DC motor drives*. CRC press, 2017.

[16] Adeeb Ahmed. *Maximum torque per ampere (mtpa) control for permanent magnet synchronous machine drive system*. PhD thesis, University of Akron, 2013.

[17] John Gasking. Resolver-to-digital conversion: A simple and cost effective alternative to optical shaft encoders. *Application Note AN*, 263, 1992.

[18] The MathWorks Inc. Matlab version: 9.13.0 (r2022b), 2022. URL: `https://www.mathworks.com`.

[19] URL: `https://www.mathworks.com/help/sps/powersys/ref/permanentmagnetsynchronousmachine.html?s_tid=doc_ta`.

[20] URL: `https://www.mathworks.com/help/sps/powersys/ref/twolevelconverter.html?s_tid=doc_ta`.

[21] URL: `https://www.mathworks.com/help/sps/ref/pwmgeneratorthreephasetwolevel.html?searchHighlight=PWM+generator&s_tid=srchtitle_support_results_5_PWM%2520generator`.

[22] Simulink Documentation. Simulation and model-based design, 2020. URL: `https://www.mathworks.com/products/simulink.html`.

[23] URL: `https://www.mathworks.com/help/sps/ref/pmsmcurrentcontroller.html?s_tid=doc_ta`.

[24] Dongshu Wang, Dapei Tan, and Lei Liu. Particle swarm optimization algorithm: an overview. *Soft computing*, 22:387–408, 2018.

[25] Mudita Juneja and SK Nagar. Particle swarm optimization algorithm and its parameters: A review. In *2016 International Conference on Control, Computing, Communication and Materials (ICCCCM)*, pages 1–5. IEEE, 2016.